LOCKHEED MARTIN ENERGY RESEARCH LIBRARIES
3 4456 0449167 2

CENTRAL RESEARCH LIBRARY
ORNL-TM-4526

Cy 1

IRRADIATION PERFORMANCE OF HTGR FUEL RODS IN HFIR EXPERIMENT HRB-3 AND ETR EXPERIMENT P13N

F. J. Homan

J. H. Coobs
R. L. Hamner
J. A. Conlin
B. H. Montgomery
E. L. Long, Jr.
J. L. Scott

OAK RIDGE NATIONAL LABORATORY
CENTRAL RESEARCH LIBRARY
DOCUMENT COLLECTION
LIBRARY LOAN COPY
DO NOT TRANSFER TO ANOTHER PERSON
If you wish someone else to see this document, send in name with document and the library will arrange a loan.
UCN-7969
(3 3-67)

OAK RIDGE NATIONAL LABORATORY
OPERATED BY UNION CARBIDE CORPORATION • FOR THE U.S. ATOMIC ENERGY COMMISSION

Printed in the United States of America. Available from
National Technical Information Service
U.S. Department of Commerce
5285 Port Royal Road, Springfield, Virginia 22151
Price: Printed Copy $5.45; Microfiche $1.45

This report was prepared as an account of work sponsored by the United States Government. Neither the United States nor the United States Atomic Energy Commission, nor any of their employees, nor any of their contractors, subcontractors, or their employees, makes any warranty, express or implied, or assumes any legal liability or responsibility for the accuracy, completeness or usefulness of any information, apparatus, product or process disclosed, or represents that its use would not infringe privately owned rights.

LOCKHEED MARTIN ENERGY RESEARCH LIBRARIES

3 4456 0449167 2

ORNL-TM-4526
(UC-77 Gas-Cooled
Reactor Technology)

Contract No. W-7405-eng-26

METALS AND CERAMICS DIVISION

REACTOR DIVISION

IRRADIATION PERFORMANCE OF HTGR FUEL RODS IN HFIR EXPERIMENT HRB-3 AND ETR EXPERIMENT P13N

F. J. Homan

J. H. Coobs J. A. Conlin E. L. Long, Jr.

R. L. Hamner B. H. Montgomery J. L. Scott

OCTOBER 1974

OAK RIDGE NATIONAL LOABORATORY
Oak Ridge, Tennessee 37830
operated by
UNION CARBIDE CORPORATION
for the
U.S. ATOMIC ENERGY COMMISSION

CONTENTS

	Page
Abstract	1
Introduction	1
Description of Capsule HRB-3 and Fuel Specimens	3
Capsule	3
Fuel	5
Loading Scheme	5
Coated Particles	6
Design of the Fissile Particles for HRB-3	6
Fuel Rods	8
Experiment HRB-3 Irradiation	10
Irradiation Conditions	10
Capsule Operation	12
Fuel Specimen Temperature	19
Postirradiation Examination and Analysis of HRB-3	23
Disassembly and Visual Examination	23
Dimensional and Weight Changes	25
Metallographic Examination	29
Specimen 1D	29
Specimen 1E	31
Specimen 3A	31
Fissile Particle Behavior	35
ORNL Specimens from ETR Capsule P13N	37
Fabrication	39
Irradiation	41

Postirradiation Examination 46

Physical Examination 46

Metallographic Examination 48

Electron-Microprobe Analysis 53

Comparison of Results in HRB-3 and P13N. 57

Discussion 57

Conclusions. 59

Acknowledgments. 60

IRRADIATION PERFORMANCE OF HTGR FUEL RODS IN HFIR EXPERIMENT HRB-3 AND ETR EXPERIMENT P13N

F. J. Homan

J. H. Coobs, J. A. Conlin,[1] E. L. Long, Jr.,

R. L. Hamner, B. H. Montgomery,[1] and J. L. Scott

ABSTRACT

Strong-acid-resin fissile particles and thoria fertile particles were irradiated in HFIR experiment HRB-3 and ETR experiment P13N. The fuel irradiated in the P13N experiment was fully enriched (90.8% ^{235}U); the fuel irradiated in HRB-3 was 7.35% enriched. The fuel from both experiments performed well, considering the high operating temperatures. There was some attack of the inner LTI and SiC coatings by fission products in HRB-3, especially in the slug-injected specimens. The attack was not temperature gradient dependent. Migration of the ThO_2 fertile particle kernels was noted for the first time in the HRB-3 experiment. A small amount of migration was noted in the warm-molded specimens, but the migration was more pronounced in the slug-injected specimens with lower matrix density. In the P13N specimens considerable kernel migration was noted in the fissile particles, to the extent that numerous failures were seen. However, there was no migration of the ThO_2. These observations and data from previous experiments have led us to the tentative conclusion that kernel migration has threshholds in temperature, temperature gradient, and burnup; and that once the threshholds are exceeded migration may occur very rapidly. The importance of the time parameter on kernel migration has not yet been fully evaluated. Data from real-time tests will be compared with data from accelerated tests such as HRB-3 and P13N to provide insight into the influence of this important parameter.

INTRODUCTION

The HRB-3 experiment is the third in a series of HTGR fuel irradiations conducted in the removable beryllium (RB) reflector facility of

[1]Reactor Division

the High Flux Isotope Reactor (HFIR). As indicated in earlier work,[2,3] HTGR fuel consists of beds of closely packed coated particles, containing uranium as the fissile material and thorium as the fertile material. The particles are bonded into fuel rods with a carbonaceous binder. The fuel kernels are coated with layers of porous and dense pyrolytic carbon, and sometimes silicon carbide. Production fuel rods are irradiated in large blocks of graphite. Experimental fuels are irradiated in graphite sleeves to simulate these blocks. The first experiment in this series, HRB-1, was designed to study the interaction of the particle coatings, matrix material, and graphite block during irradiation.[2] The second experiment, HRB-2, was designed to study the performance of preproduction Fort St. Vrain[4] fuel to peak fast neutron exposure, and to test the performance of early-production Triso[5] fissile and fertile particles.

The objectives of the HRB-3 experiment were:

1. To test continuous matrix fuel rods made at ORNL at two volume loadings of particles, 33 and 42%. Primarily it was desired to correlate dimensional behavior with composition and fluence.
2. To test slug-injected fuel rods to full fluence. These rods were fabricated at ORNL by the technique currently planned for use in refabrication of fuel in the recycle pilot plant.
3. To test fuel rods fabricated by General Atomic Company (GAC) as prototype rods for reference 1160-MW(e) reactor design. These rods contained oxide fuel kernels.
4. To measure the thermal conductivity of a continuous-matrix fuel rod.
5. To calibrate tungsten-rhenium alloy thermocouples for use at elevated temperatures and determine the effects of radiation damage on their thermoelectric output.

The first four objectives listed above were achieved, and valuable information on the decalibration of tungsten-rhenium alloy thermocouples in a neutron flux was obtained. Absolute calibration of the thermocouples was not achieved, however.

---

[2]J. L. Scott, J. A. Conlin, J. H. Coobs, D. M. Hewette II, J M Robbins, R. L. Senn, and B. H. Montgomery, *An Irradiation Test of Bonded HTGR Coated Particle Fuels in an Instrumented Capsule in HFIR*, ORNL-TM-3640 (March 1972).

[3]J. H. Coobs, J. L. Scott, B. H. Montgomery, J M Robbins C. B. Pollock, and J. A. Conlin, *Irradiation Performance in HFIR Experiment HRB-2 of HTGR Fuel Sticks Bonded with Reference and Advanced Matrix Materials*, ORNL-TM-3988 (January 1973).

[4]The Fort St. Vrain Reactor is a 330-MW(e) HTGR Demonstration Reactor built by Gulf General Atomic for Public Service of Colorado.

[5]Triso fuel consists of a fuel kernel coated successively with a porous layer of pyrolytic carbon, a dense layer of pyrolytic carbon, a dense layer of silicon carbide, and a second dense layer of pyrolytic carbon.

The irradiation behavior of fuel rods fabricated at ORNL and irradiated in ETR experiment P13N is also reported here. This fuel was very similar to the fuel irradiated in HRB-3. The fissile particles in both experiments were strong-acid-resin-derived UCS coated with Triso coatings but without a buffer layer. The uranium in the fissile particles was 7.35% enriched in HRB-3 and fully enriched in P13N. The fertile particles were from the same batch in both experiments, and the matrix materials were also identical.

DESCRIPTION OF CAPSULE HRB-3 AND FUEL SPECIMENS

Capsule

Instrumented capsule HRB-3 was similar in design to the first two HRB capsules.[2,3] The dimensions of the primary and secondary containment and of the graphite sleeve were somewhat different. The test fuel was different, and one specimen contained a center-line thermocouple, which was not included in the earlier tests. A cross section of the capsule is shown in Fig. 1. It was a double-walled water-cooled stainless steel vessel. The outer capsule (secondary containment) had an OD of 1.292 in. and an ID of 1.140 in. The primary containment had OD and ID of 1.137 and 0.9676 in., respectively. The test fuel specimens consisted of a series of 0.490-in.-diam bonded fuel rods having a total stack length of 15.3 in. The specimens were supported in a one-piece sleeve made of Poco graphite, grade AXF-5Q. The design test conditions of 1250°C peak fuel temperature at 5.5 kW/ft (fission plus gamma heat in the fuel specimens) were intended to match conditions typical in a large HTGR.

Temperatures were monitored by nine sheathed 0.062-in.-diam thermocouples (eight Chromel vs Alumel and one W–3% Re vs W–25% Re) and one bare wire W–3% Re vs W–25% Re central thermocouple. The stainless-steel-sheathed thermocouples were coated with a 0.005-in.-thick protective barrier of chemically vapor deposited tungsten and were located in axial holes in the graphite sleeve adjacent to the fuel specimens (see Fig. 2). The central thermocouple lead wires were threaded through a two-hole 0.062-in.-diam BeO insulator. The junction and lower 2 in. of the insulator were shielded from the fuel surface by three layers of 0.0025-in.-thick rhenium foil. The upper fuel specimens 1A through 1F (see Fig. 2) were made with a 0.090-in. central hole for this thermocouple. Titanium and iron flux monitor wires, enclosed in three platinum tubes, were located in the graphite sleeve in axial holes similar to those for the thermocouples. The graphite sleeve and the fuel specimens were continuously swept with 3600 cm^3/hr of high-purity helium-neon mixture at 1 to 2 atm. Gas samples of the sweep effluent were taken periodically for fission gas release determinations.

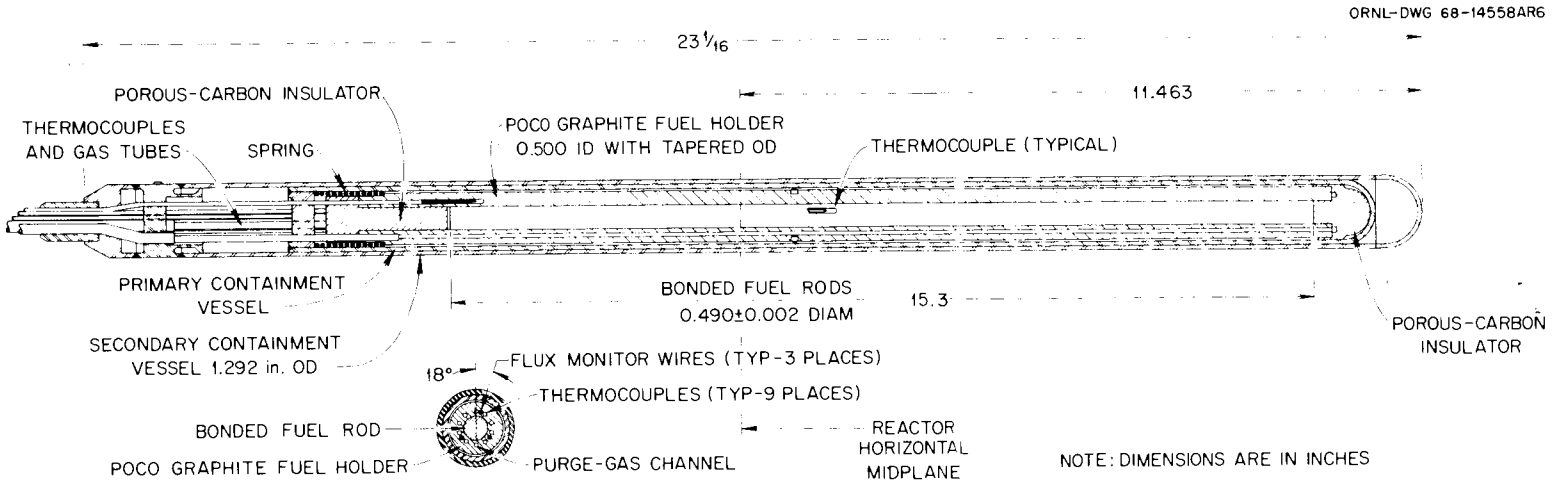

Fig. 1. Cross Section of HTGR Instrumented Capsule HRB-3.

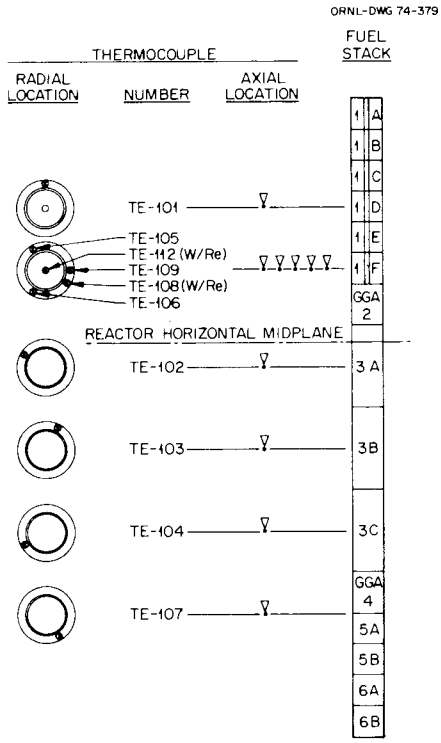

Fig. 2. HRB-3 Fuel Specimen and Thermocouple Locations.

Fuel

Loading Scheme

Fifteen fuel rod specimens were irradiated in HRB-3. Two of the specimens were fabricated by General Atomic Company, the reaminder by ORNL. The loading scheme for the capsule is shown in Fig. 3. The GAC specimens (indicated by GGA in the figure) were fabricated and examined at GAC and will not be discussed further in this report. Three of the ORNL specimens (3A, 3B, 3C) were formed by slug injection[6] and had high particle volume fractions (typically about 60 vol % particles). The remainder of the ORNL specimens were warm molded. The warm molding process yields a continuous, relatively high-density matrix with thermal conductivity considerably higher than that of the slug-injected matrix. As indicated in Fig. 3, six of the ORNL specimens had central holes for thermocouple placement. Of the ten specimens fabricated at ORNL by the warm molding process, five had particle volume fractions of about 33% (specimens 1A, 1C, 1E, 5A, 6A). The remainder had particle volume fractions of about 42%.

---

[6]R. A. Bradley, C. F. Sanders, and D. D. Cannon, "Fuel Stick Preparation," *Gas-Cooled Reactor and Thorium Utilization Programs Annu. Progr. Rep. Sept. 30, 1971*, ORNL-4760, pp. 52–55.

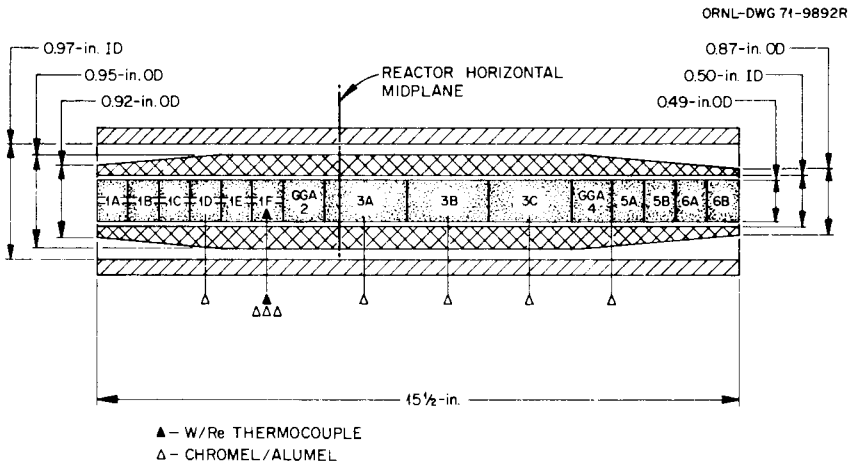

Fig. 3. HRB-3 Configuration.

Coated Particles

All specimens prepared at ORNL contained coated particles from the same batches except that warm-molded specimens having the lowest particle volume loading did not contain diluent particles. The slug-injected specimens contained Triso-coated fissile UCS particles of low enrichment derived from strong-acid resin, Biso-coated ThO_2 derived by the sol-gel process, and Triso- and Biso-coated carbon diluent particles derived from desulfurized strong-acid resin. The diluent particles were used in the same volume ratio as that for the fissile and fertile particles to obtain a more realistic simulation of the size of heavy metal particles. All particles were heat treated at 1800°C for 30 min to relieve residual stresses that might result in broken coatings during the fuel rod fabrication process. Characterization of the coated particles is given in Table 1. Deposition conditions for the coatings are given in Table 2.

Design of the Fissile Particles for HRB-3

In the design of the fissile particles for HRB-3 we sought to exploit the advantages of fuel kernels derived from strong-acid resins. Since the overall kernel density is only 2.73 g/cm^3 and a kernel contains slightly over 50 wt % U in the from US, the fuel occupies only 16% of the kernel volume. The carbon content is slightly over 37 wt %, and it occupies 48.5% of the kernel volume after it densifies, if one assumes that its final density is 2.0 g/cm^3. This densification occurs rapidly and is activated by fission recoils. The assumed density is equivalent to that observed for pyrolytic carbon coatings after irradiation. The remaining volume, 35.5% is sufficient to accommodate fuel swelling expected for full burnup of fully enriched fuel. Consequently, no buffer is needed to provide void volume for fuel swelling and fission-gas release. To be sure, a buffer was originally thought to be required in the early days to prevent fission recoil damage to the outer coatings. We reckoned, however, that

Table 1. Characterization of Coated Particles for HRB-3

Batch	Kernel Material	Layer	Dimension[a,b] (μm)	Density[b,c] (g/cm^3)
OR-1627-28[d]	UCS[e]	Kernel	431 ± 32	2.73
		Inner LTI	22 ± 3	1.8[f]
		SiC	23 ± 1	3.21 ± 0.0012
		Outer LTI	63 ± 8	1.86 ± 0.0212
OR-1666-19[g]	UCS[e]	Kernel	412.0 ± 47.7	2.7
		Inner LTI	24 ± 3.0	1.8[f]
		SiC	25.0 ± 1.2	3.23 ± 0.005
		Outer LTI	55.1 ± 3.7	2.07 ± 0.008
OR-1562[h]	ThO_2	Kernel	398 ± 17	9.9
		Buffer	55 ± 8	1.2[f]
		Outer LTI	76 ± 6	1.97 ± 0.007
OR-1596-99	Carbon[i]	Kernel + inner	437 ± 26	1.3
		SiC	20 ± 1	3.23 ± 0.006
		Outer LTI	58 ± 8	1.93 ± 0.013
OR-1577-78-80	Carbon[i]	Kernel	484 ± 33	
		Buffer	44 ± 7	1.0[f]
		Outer LTI	75 ± 7	1.93 ± 0.004

[a]Diameter of kernels, thickness of coatings.

[b]Mean value ± standard deviation.

[c]Kernel density measured after final stage of processing just before annealing. SiC and outer LTI densities determined by density-gradient column method before anealing.

[d]Used in warm-molded rods; contains 17.0 wt % U enriched to 7.35 at. % ^{235}U.

[e]Derived from strong acid resin; composition 50.7% U, 37.8% C, 9.77% S in batch OR-1627-28; 53.8% U, 37.9% C, 7.06% S in batch OR-1666-19.

[f]Estimated from coating conditions.

[g]Used in slug-injected rods; contains 14.4 wt % U enriched to 7.35 at. % ^{235}U.

[h]Contains 51.6% Th in sol-gel-derived ThO_2 kernels.

[i]Derived from strong acid resin. Desulfurized by heating at 2600°C for 30 min.

Table 2. Average Coating Deposition Rates for HRB-3 Experiment

Layer	Deposition		Deposition rate, μm/min, for Batch OR-				
	Gas	(°C)	1627-28	1666-19	1562	1596-99	1577-78-80
Buffer	C_2H_2	1050			10.9		9.57
Inner LTI	C_3H_6	1350	7.7	6.9		5.93	
SiC	CH_3SiCl_3 CH_3SiCl_2H	1550	0.4	0.16		0.21	
Outer LTI	C_3H_6	1300	9.8	7.3	6.2	6.9	4.75

since the early generation coatings were not stable relative to fast neutrons either, the present generation pyrolytic carbon coatings would be resistant to recoil damage also. As it turned out, this assumption was optimistic.

Fuel Rods

General fabrication data for ORNL specimens are given in Table 3. The three specimens prepared by slug-injection were essentially identical. The matrix used was the reference for the Fort St. Vrain Reactor — 28.5 wt % Asbury 6353 natural flake graphite powder and Allied grade 15V pitch. The matrix was injected through the particle bed at 150°C and at a pressure of 1000 psi. The matrices were carbonized by heating the fuel rods to 800°C in a packed bed of alumina powder and then stabilized by heat treatment at 1800°C for 30 min.

Table 3. Fabrication Data for ORNL Fuel Rod Specimens Irradiated in HRB-3 Experiment

Specimen Positions	Mode of Fabrication	Matrix Materials		Mode of Carbonization
		Fillers	Binders	
1A, C, E 1B, D, F 5A, 5B 6A, 6B	Slurry blended and warm molded	53.5 wt % GLCC 1074[a] 15.0 wt % Thermax[b]	31.5% A240 pitch[c]	In packed bed of graphite powder
3A. B. C	Slug injected	28.5 wt % Asbury NF 6353[d]	71.5 wt % Allied 15V pitch[e]	In packed bed of alumina

[a]Isotropic graphite powder from Great Lakes Carbon Corporation.

[b]Spherical carbon black from R. T. Vanderbilt Company.

[c]Petroleum pitch from Ashland Oil Company.

[d]Natural flake graphite powder from The Asbury Graphite Mills.

[e]Coal tar pitch from Allied Chemical Company.

Isotropic filler materials were chosen for the specimens fabricated by warm molding (GLCC grade 1074 graphite powder and Thermax) in order to obtain a reasonably isotropic matrix for irradiation resistance. Ashland grade 240 pitch (A 240) was chosen as binder because of its relatively low melting point (~120°C) and its amenability to the fabrication process. All components were slurry blended in a mixture of toluene and acetone. These solvents were selected because, in combination, they aided in coating the coated particles with the matrix materials and in granulation of the mix for forming. After evaporation of the solvent, the granulated mix was pressed in a steel die at 165°C at a pressure of 1000 psi. The specimens with thermocouple holes were formed by use of a steel mandrel extending through the punches and the coated particle-matrix granules. After cooling to room temperature, the specimens were carbonized by heating to 1000°C for 24 hr in a packed bed of graphite powder, then heat-treated at 1800°C for 30 min.

Physical characteristics and heavy metal loadings for the specimens are given in Table 4 and 5. The matrix densities for the warm-molded specimens were relatively high (average 1.48 g/cm^3). The matrix densities for the slug-injected specimens were low (average 0.60 g/cm^3), but this was as expected because of the high particle volume loading (~ 60%) and the large amount of pitch in the matrix material.

The fuel loadings were increased at the lower end of the capsule, as shown in Table 5, to compensate for the lower neutron flux and in the upper end for the loss of volume due to the central thermocouple hole. Because of the high thermal flux in the HFIR-RB facility, the ^{235}U is

Table 4. Physical Characteristics of Fuel Rod Specimens Irradiated in HRB-3 Experiment

Specimen	Position in Capsule	Average OD[a] (in.)	Length, in.		Particle Volume Loading (%)	Matrix Density (g/cm^3)
			Specified	Average		
JH-206-3	1A	0.4876	0.75	0.7495	32.7	1.49
JH-214-3	1B	0.4886	0.75	0.7527	41.6	1.47
JH-214-1	1C	0.4887	0.75	0.7499	32.5	1.48
JH-206-4	1D	0.4888	0.75	0.7512	41.6	1.46
JH-210-4	1E	0.4898	0.75	0.7468	32.5	1.47
JH-214-2	1F	0.4888	0.75	0.7508	41.6	1.47
M58A71	3A	0.4925	2.00	1.9772	59.7	0.601
M58A73	3B	0.4925	2.00	1.9910	59.4	0.610
M58A75	3C	0.4922	2.00	1.9852	59.5	0.602
JH-199-1	5A	0.4877	0.70	0.6976	32.7	1.48
JH-199-2	5B	0.4890	0.70	0.7021	41.6	1.47
JH-199-3	6A	0.4880	0.70	0.6971	32.7	1.49
JH-199-4	6B	0.4891	0.70	0.7009	41.6	1.47

[a]Specified outside diameter for all specimens: 0.490 ± 0.002 in. Specimens for positions 1A through 1F met within the accuracy of measurement the specified inside diameter of 0.091 in. All other specimens were solid.

Table 5. Fuel Loading for HRB-3 Experiment

Specimen Position	Fuel Loading, g/cm^3		
	^{235}U	^{238}U	^{232}Th
1A	0.0065	0.0814	0.1583
1B	0.0064	0.0807	0.1569
1C	0.0064	0.0810	0.1575
1D	0.0064	0.0809	0.1572
1E	0.0064	0.0807	0.1574
1F	0.0064	0.0809	0.1572
3A	0.0052	0.0659	0.1283
3B	0.0052	0.0655	0.1283
3C	0.0052	0.0658	0.1276
5A	0.0053	0.0678	0.1316
5B	0.0053	0.0669	0.1301
6A	0.0063	0.0815	0.1585
6B	0.0065	0.0806	0.1568

consumed rapidly (50% in about 16 days at the reactor midplane). Continuing fissiong power in the fuel specimens was provided by the ^{232}Th and ^{238}U, which convert to fissile material by neutron capture.

The capsule was designed to obtain reasonably uniform axial temperatures by tapering the graphite sleeve so as to increase the gas gap between the graphite and the capsule wall, thus varying the thermal resistance between the graphite sleeve and water-cooled capsule inversely with the calculated initial axial power. To compensate for overall power variations with time, the composition of the helium-neon sweep gas mixture, which occupied the gap, was varied to maintain the peak fuel temperature at the design level.

EXPERIMENT HRB-3 IRRADIATION

Irradiation Conditions

The HRB-3 experiment was irradiated in the RB-5 facility of the HFIR Core. The location of this facility is shown in Fig. 4. This facility is characterized by a fairly steep radial gradient of fast neutron

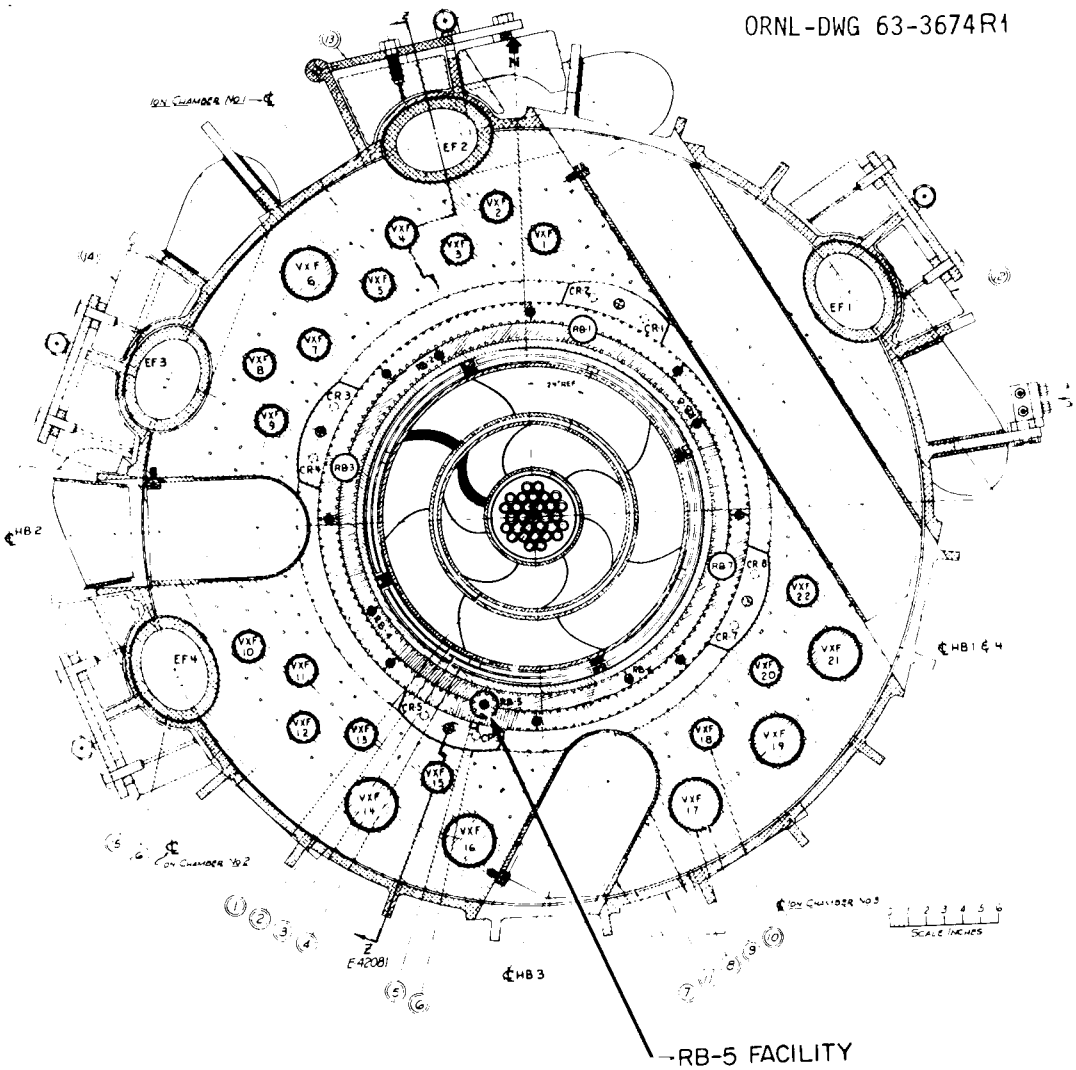

Fig. 4. HFIR Cross Section at Horizontal Midplane.

flux but a fairly constant thermal neutron flux, as shown in Fig. 5. Notice, in Fig. 5, that the thermal flux is somewhat lower in the clean core (beginning of the 23-day irradiation cycle) than after 21 days of irradiation. This characteristic of the HFIR RB facility is quite important to the operation of the HRB capsules, as will be explained in detail later in this report. The reason for this increase in flux with irradiation time in the RB facility is the change in the position of the control rods. At the beginning of the irradiation the control rods are fully inserted, as shown in Fig. 6. As the core fuel is burned out the control rods are moved away from the horizontal midplane of the reactor, increasing the neutron fluxes in all regions of the core. This is necessary to maintain a constant 100 MW of reactor power with the rapid depletion of fissile fuel in the fuel elements. The axial thermal flux profiles at the beginning and end of a 23-day irradiation cycle are shown in

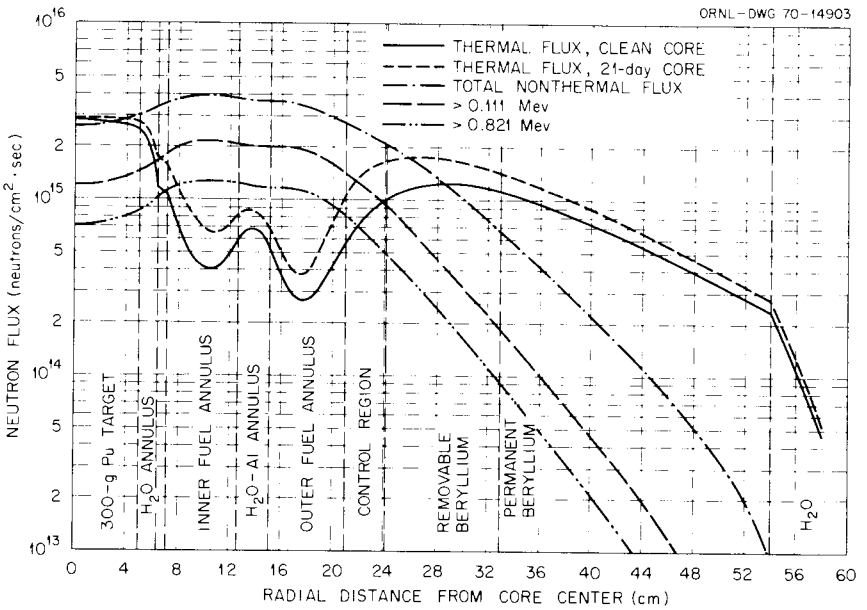

Fig. 5. Typical Radial Neutron Flux Distributions at Core Horizontal Midplane with Reactor Operating at 100 MW.

Fig. 7. The increase in thermal neutron flux with time is shown in Fig. 8 for the reactor midplane.

Gamma heating is an important component of heat generation in the HRB capsules. Gamma heating rates are significant in both the graphite sleeve and the stainless steel capsule, as shown in Figs. 9 and 10. As indicated earlier, this experiment was designed so that the fuel generated 5.5 kW/ft (fission energy plus gamma heat in the fuel). Using the data in Figs. 9 and 10 shows that about 80% of the heat from the capsule is derived from gamma heating in the graphite and stainless steel.

The coolant water in the HFIR core flows downward. It enters the core at about 120°F. The exit temperature in the target region[7] is about 196°F, and the exit temperature from the RB region is about 150°F.

Capsule Operation

Capsule HRB-3 was inserted in the HFIR removable beryllium facility (RB-5) on January 6, 1972, and was irradiated for 11 HFIR fuel cycles — 253.75 days at 100 MW reactor power (271 days in the reactor). The irradiation was completed and the capsule removed as scheduled on October 4, 1972. Capsule operation was stable throughout the irradiation, and all test parameters were within design limits. There was as expected an initial drop in power as the ^{235}U was consumed, followed by a gradual power buildup, which varied with time, axial position, and

[7]R. D. Cheverton and T. M. Sims, *HFIR Core Nuclear Design*, ORNL-4621, (July 1971), p. 3.

ORNL-DWG 63-8100R

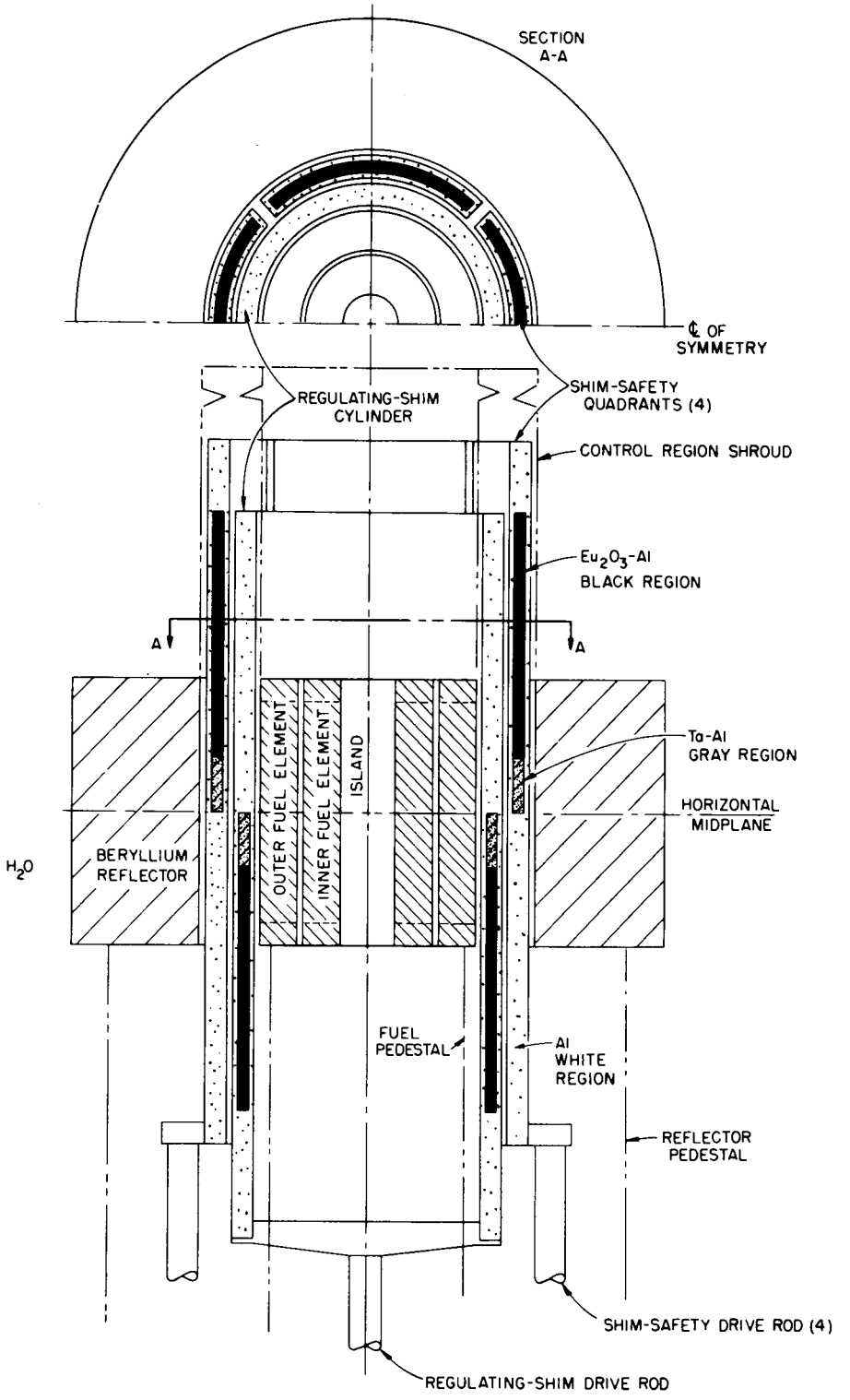

Fig. 6. Schematic Representation of HFIR Core.

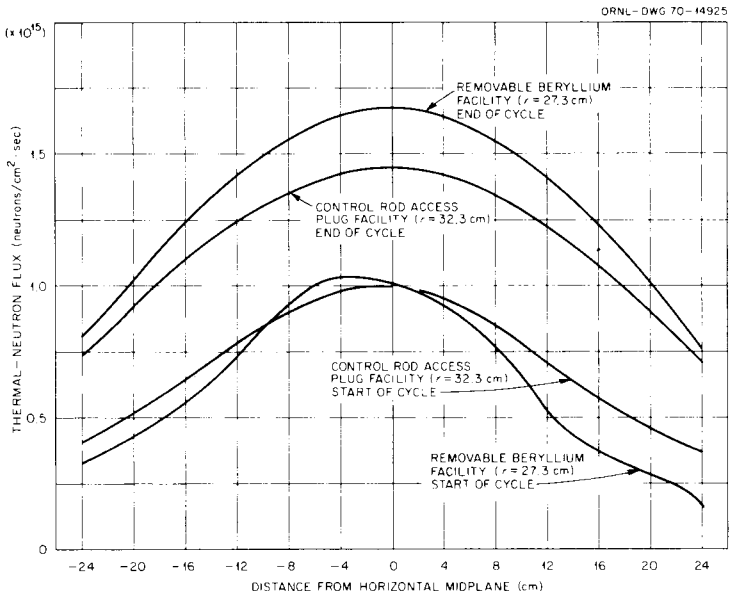

Fig. 7. Thermal Flux Axial Profiles in Removable Beryllium Reflector Experiment Facilities at 100 MW.

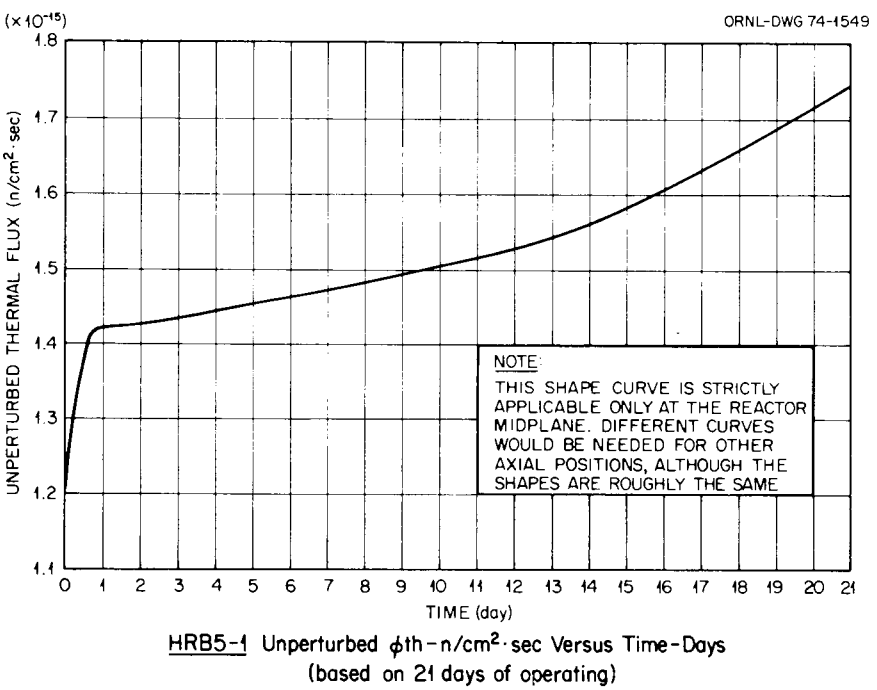

Fig. 8. Increase in Thermal Neutron Flux During a Reactor Cycle.

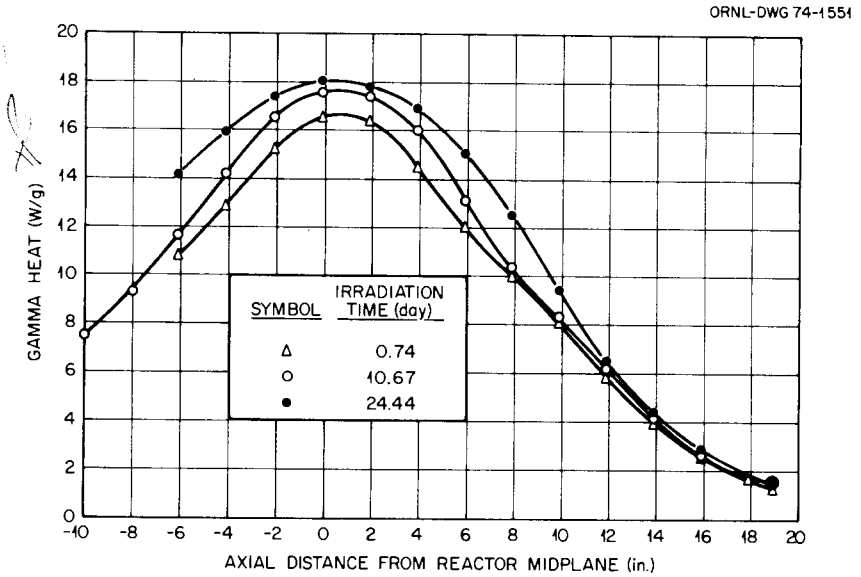

Fig. 9. Measured Axial Distribution of Stainless Steel Heat Generation in the HFIR RB-5 Facility.

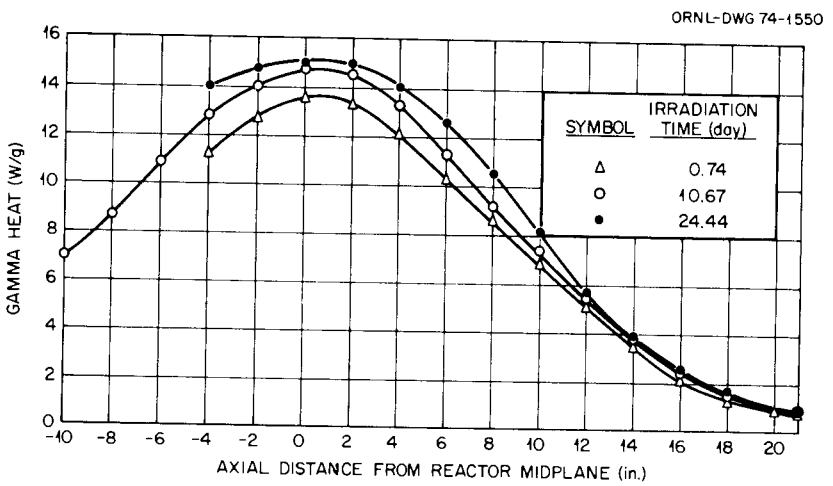

Fig. 10. Measured Axial Distribution of Graphite Heat Generation in the HFIR RB-5 Facility.

fuel loading. This is shown graphically in Fig. 11, which presents the calculated fission power generated by specimens 1D, 1E, 1F, and 3A.

The calculated isotopic burnup and neutron fluence along with fuel loadings for each sample are shown in Table 6. These calculations were based on a peak (reactor horizontal midplane) fast (>0.18 MeV) flux of 5×10^{14} neutrons cm^{-2} sec^{-1} and a perturbed thermal (<0.41 eV) flux of 1.18×10^{15} neutrons cm^{-2} sec^{-1}.

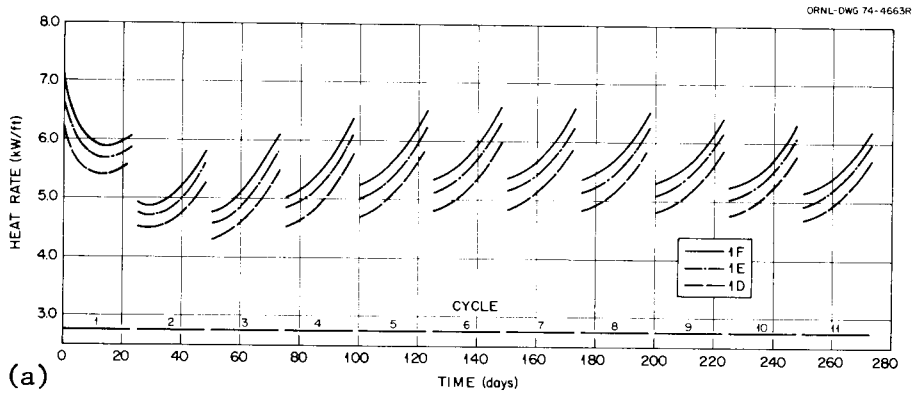

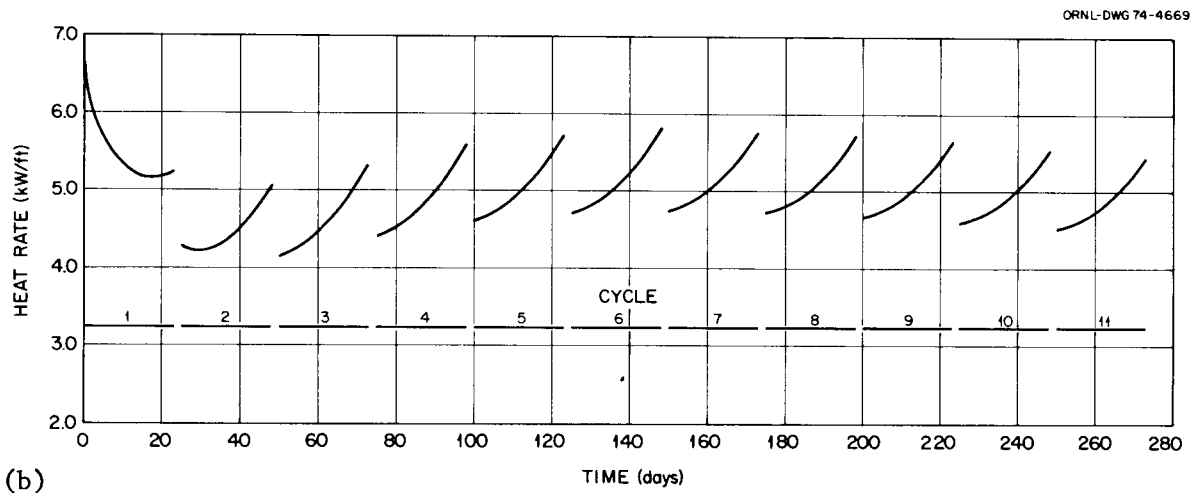

Fig. 11. Heat Rate Versus Time for HRB-3 Specimens, (a) 1F, 1E, and 1D. (b) 3A.

The helium-neon sweep gas effluent was sampled periodically to measure fission gas release. The ratios of release rate to birth rate (R/B) of selected isotopes are shown as a function of accumulated irradiation time in Fig. 12. The birth rates used in this calculation take into account the depletion of ^{235}U and the buildup of ^{233}U and ^{239}Pu. We first calculated the daily change in isotopic composition of the fuel for each specimen and then the fission product yield from each fissionable isotope. The R/B ratios increased on day 59 because of an intentional increase in capsule temperatures. After day 79 we had to change gamma ray spectrometer equipment because of the high radiation level in the sweep gas samples. For an interim period between day 83 and day 106 the alternate system indicated R/B ratios higher than those obtained earlier. This is attributed to the use of different energy peaks for counting the sample activities in the two spectrometer systems. The step increase on day 83 is an artifact of the computational method, but the general increase with time is real.

Table 6. HRB-3 Specimen Loading, Burnup, and Fluence

Fuel Rod	Length (in.)	Volume (cm^3)	Fuel Loading, g/cm^3			Burnup,[a] %		Fluence, neutrons/cm^2	
			^{235}U	^{238}U	^{232}Th	^{238}U	^{232}Th	Fast >0.18 MeV	Thermal <0.414 eV
1 A	0.7495	2.2150	0.00646	0.08144	0.15833	18.0	8.8	0.80×10^{22}	1.49×10^{22}
1 B	0.7527	2.2341	0.00640	0.08075	0.15693	20.5	10.0	0.87	1.69
1 C	0.7499	2.2267	0.00642	0.08102	0.15749	21.9	11.1	0.93	1.86
1 D	0.7512	2.2315	0.00641	0.08084	0.15720	23.0	12.2	0.98	2.03
1 E	0.7468	2.2278	0.00642	0.08098	0.15737	24.5	13.0	1.03	2.19
1 F	0.7508	2.2303	0.00641	0.08088	0.15724	25.4	13.8	1.07	2.35
GGA-2	1.0010	3.0555	0.00517	0.06683	0.12993	26.5	14.7	1.10	2.48
3 A	1.9772	6.1718	0.00522	0.06586	0.12824	26.5	15.0	1.10	2.60
3 B	1.9910	6.2155	0.00519	0.06538	0.12726	24.3	13.9	1.03	2.52
3 C	1.9850	6.1893	0.00522	0.06579	0.12764	20.2	11.8	0.89	2.21
GGA-4	0.9990	3.0490	0.00518	0.06696	0.13019	16.3	9.8	0.75	1.86
5 A	0.6976	2.1371	0.00533	0.06776	0.13158	13.5	8.2	0.66	1.63
5 B	0.7021	2.1624	0.00527	0.06696	0.13009	11.5	7.1	0.58	1.45
6 A	0.6971	2.1382	0.00645	0.08156	0.15845	9.5	5.9	0.50	1.25
6 B	0.7009	2.1595	0.00639	0.08076	0.15684	7.5	4.7	0.43	1.06

[a]In all rods, 84.0% burnup of ^{235}U.

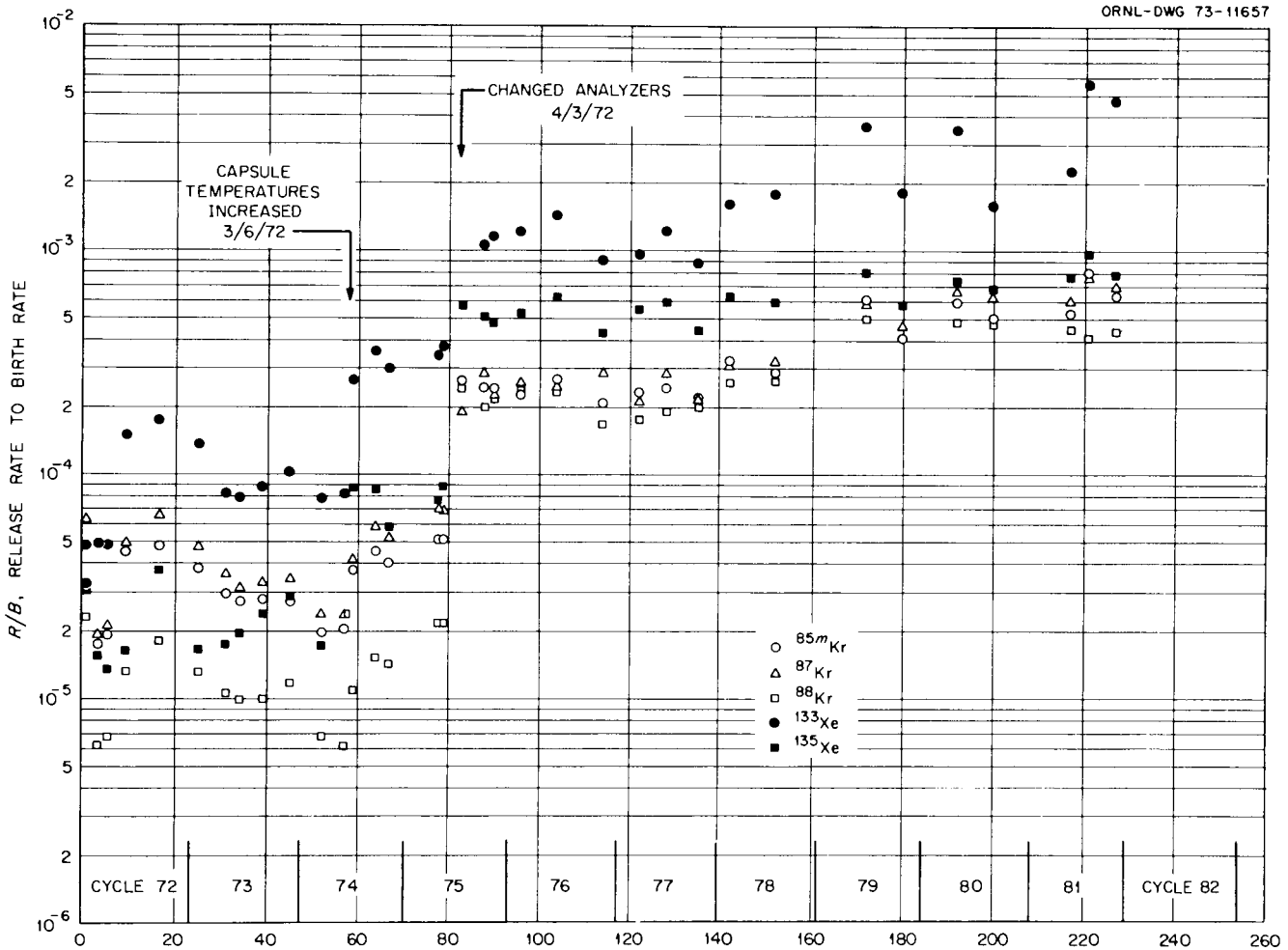

Fig. 12. Accumulated Irradiation Time — Days.

Fuel Specimen Temperature

As described previously, the HRB-3 temperatures were monitored by nine thermocouples at various axial positions in the graphite sleeve and by one central thermocouple in specimen 1F. During capsule operation, temperatures were adjusted by varying the helium-neon sweep gas mixture to adjust the gas gap thermal resistance. From the calculated fission power generation and measured graphite temperature we estimated the temperatures of all specimens and chose the specimen with the highest estimated temperature as the control point. We then adjusted the gas mixture so that the graphite thermocouple nearest this hottest specimen would be at temperature corresponding to the design central temperature (1250°C) in that specimen. In the case of HRB-3 the control thermocouple was No. 107 (adjacent to specimens GGA-4 and 5A) and was maintained at 875°C after day 59. Before day 59 the capsule had been operated with 100% helium. No attempt was made to vary the 875°C control point with time.

Figure 11 illustrates the variation of specimen fission power with time for several specimens. As can be seen specimen fission power varies with time in every cycle and gradually changes from cycle to cycle after the second cycle. The variation in the first two cycles differs from the others because of the rapid change in isotopic composition that takes place as the ^{235}U is burned out and ^{233}U and ^{239}Pu chains build in. The variation with time has a similar pattern for all specimens, but the magnitude or percent change varies from specimen to specimen. This variation is principally a function of the axial position. The percent change during a cycle increases with the distance that the specimen is from the reactor midplane and is caused by the manner in which the neutron flux changes in the HFIR with core burnout. Fuel composition also has an effect on the power-time variation, but this effect is secondary in magnitude.

Maintaining a fixed graphite temperature at one point compensates for most of the effect that this power variation has on the temperature of the specimens in the vicinity of the fixed temperature. Since the power variation with time is similar for all specimens, maintaining one point in the graphite at a fixed temperature (by adjusting the thermal resistance of the gas gap) will, to a considerable degree, compensate for the power changes in all specimens. Figures 13 through 18 illustrate the temperature history of the graphite sleeve for the sixth cycle of irradiation. Thermocouple 107 was the control point. The variation illustrated in the temperature of thermocouple 107 is a consequence of the increase in specimen fission power with time. This caused a gradual temperature increase interrupted by temperature drops when the helium-neon sweep mixture was adjusted. An examination of the other figures shows a general decrease in graphite temperature with time. This is a result of the more rapid change in fission power with time at the lower end of the capsule (near thermocouple 107). We used a 100% helium sweep for the first few days of every cycle until temperatures leveled out; hence the low temperature indicated for all thermocouples at the beginning of the cycle. The plots do not include thermocouples 104 and 108 since they had failed before the sixth cycle. Thermocouple 112 is the tungsten-rhenium alloy

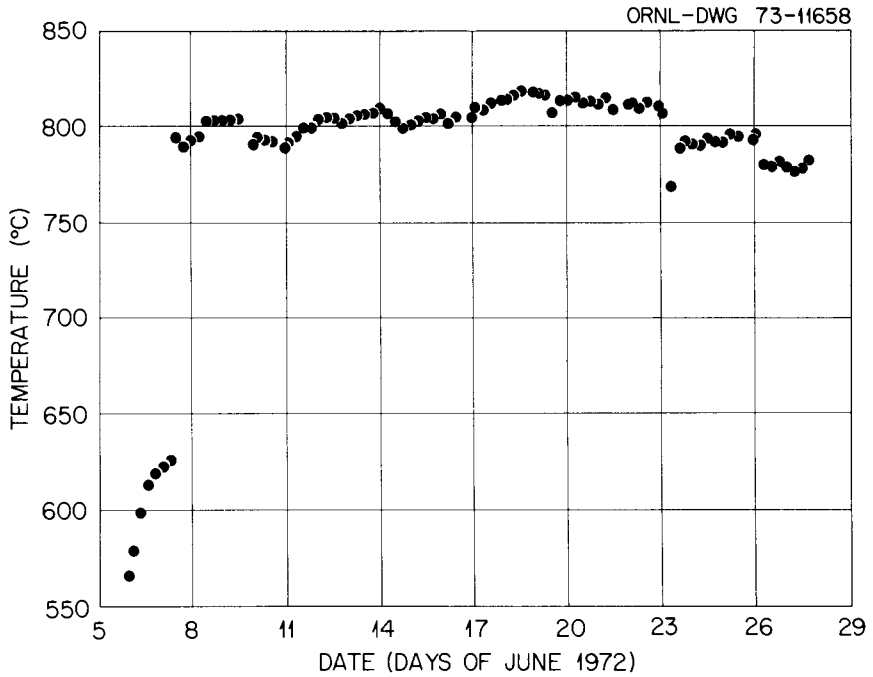

Fig. 13. Measured Temperature at Thermocouple 101 in Capsule HRB-3 During HFIR Cycle 78 (the Sixth of an 11-Cycle Irradiation).

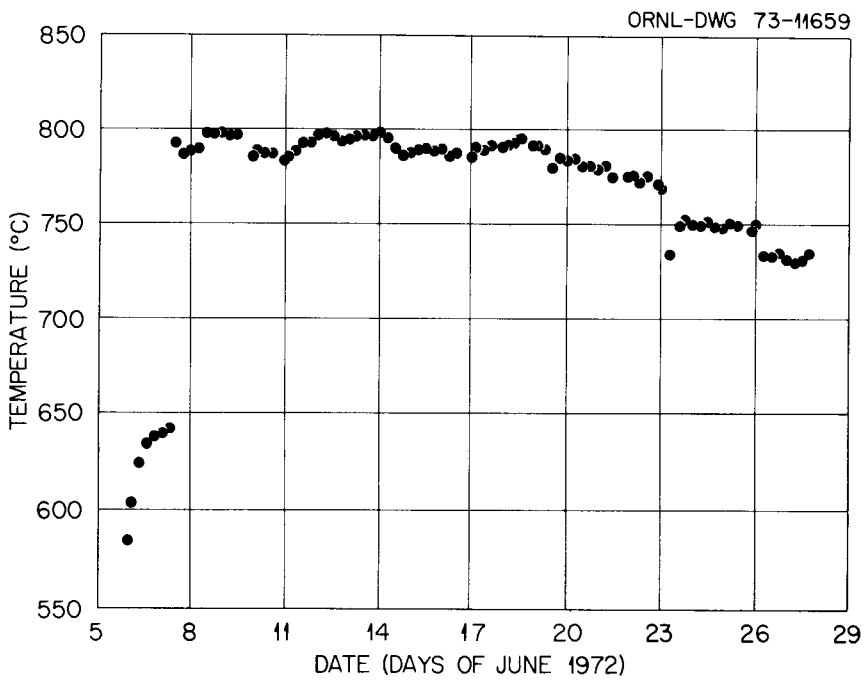

Fig. 14. Measured Temperature at Thermocouple 102 in Capsule HRB-3 During HFIR Cycle 78 (the Sixth of an 11-Cycle Irradiation).

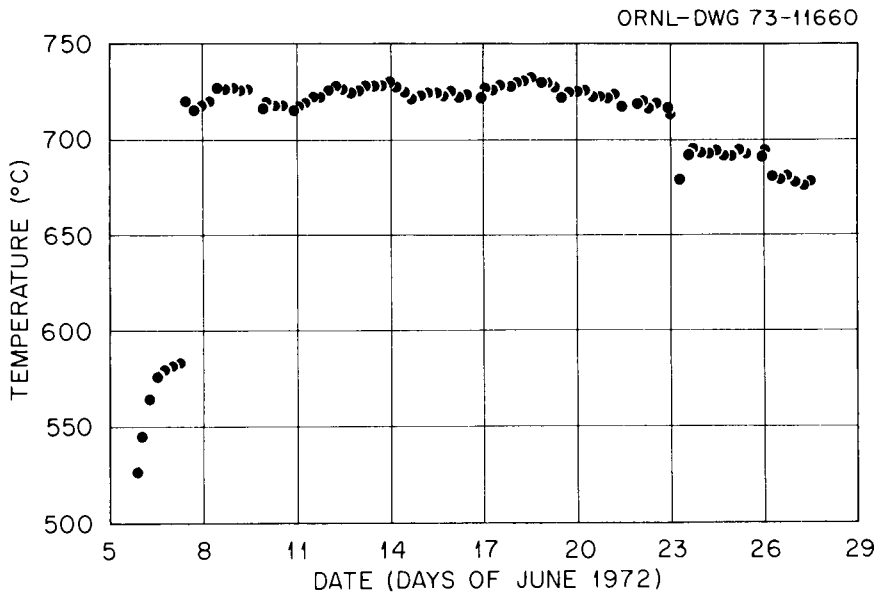

Fig. 15. Measured Temperature at Thermocouple 103 in Capsule HRB-3 During HFIR Cycle 78 (the Sixth of an 11-Cycle Irradiation).

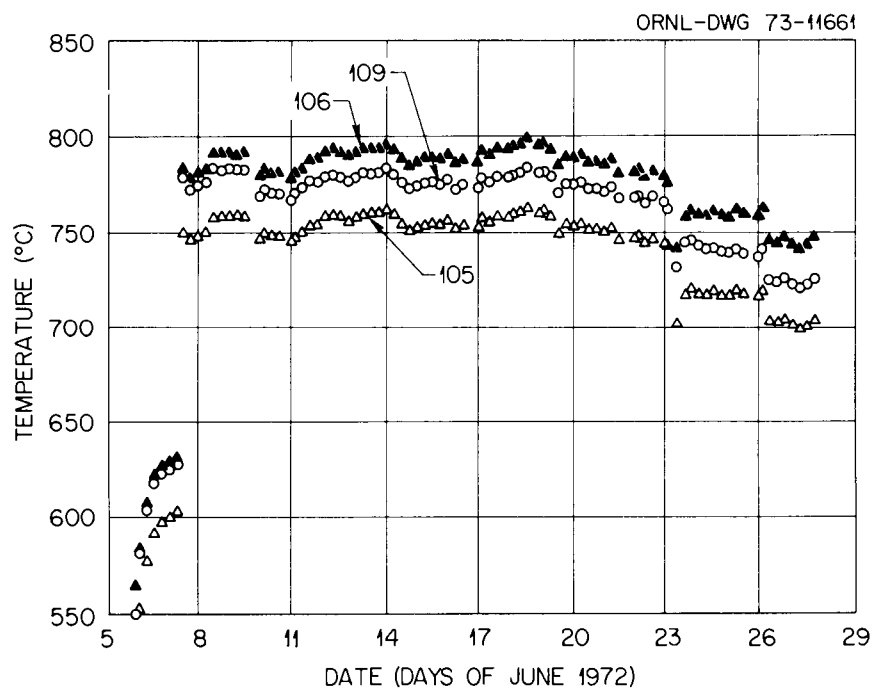

Fig. 16. Measured Temperature at Thermocouples 105, 106, and 109 in Capsule HRB-3 During HFIR Cycle 78 (the Sixth of an 11-Cycle Irradiation).

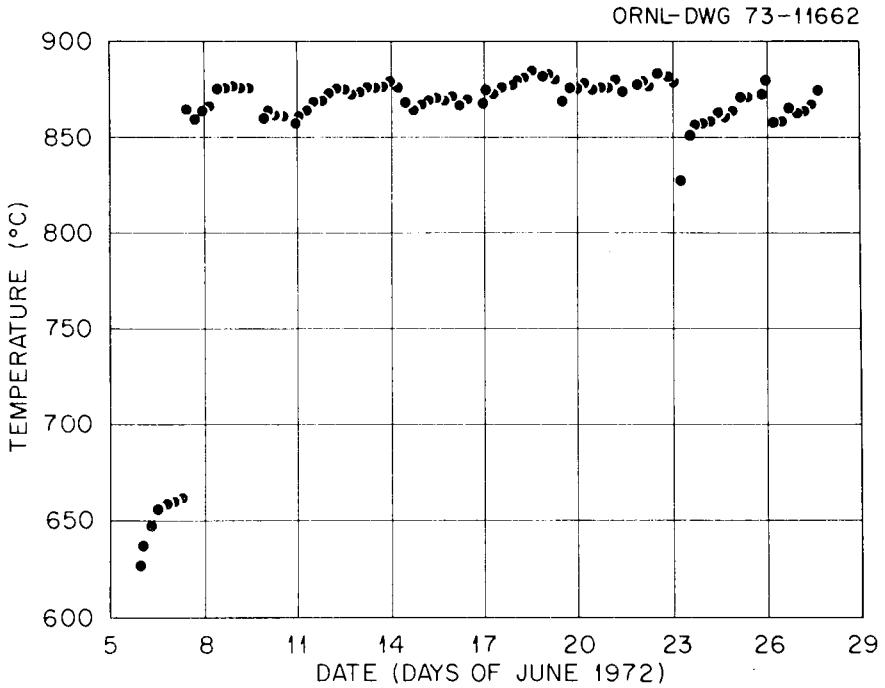

Fig. 17. Measured Temperature at Thermocouple 107 in Capsule HRB-3 During HFIR Cycle 78 (the Sixth of an 11-Cycle Irradiation).

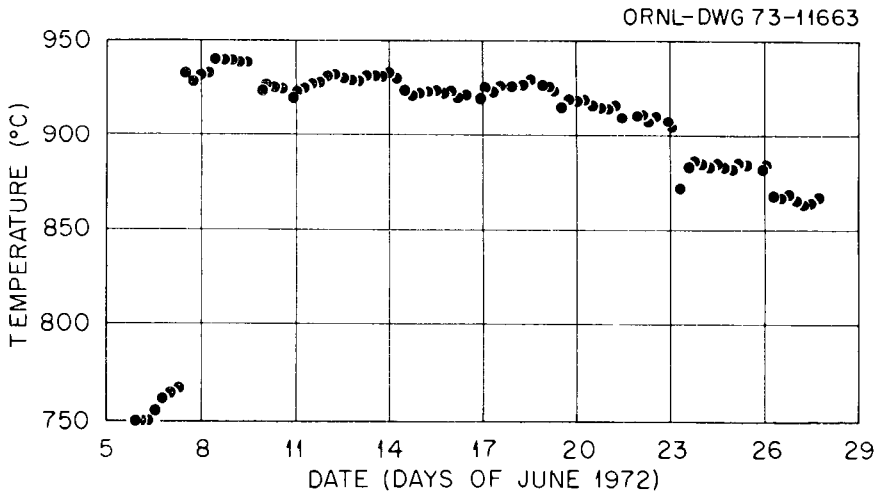

Fig. 18. Measured Temperature at Thermocouple 112 in Capsule HRB-3 During HFIR Cycle 78 (the Sixth of an 11-Cycle Irradiation).

center-line temperature sensor, which was located in specimen 1F. It decalibrated badly during the irradiation, and the values that appear in Fig. 18 do not reflect the actual operating temperatures of specimen 1F during cycle 6. The thermocouple readings must be corrected for the decalibration. This subject is covered in detail in another report.[8] Thermal analysis of this experiment includes computing the operating temperatures of the fuel, based on knowledge of the graphite sleeve temperatures (from the Chromel vs Alumel thermocouples); the thermal conductivities of the capsules, graphite sleeve, and fuel rods; the dimensional changes that occur with time in these materials; the composition of the sweep gas; and the fission and gamma heating rates. This analysis is very complex and will not be described in detail in this report; only the results will be given. The details are available in the other report.[8]

Figure 19 gives the calculated fuel center-line and surface temperatures for specimens 1D, 1F, and 3A. Specimens 1D and 3A were examined metallographically, and detailed knowledge of the operating temperatures is necessary to interpret the results. Specimen 1F is important because of the high degree of instrumentation associated with it (three Chromel vs Alumel thermocouples and two tungsten-rhenium couples), which is useful in establishing the accuracy of the thermal model and computational procedures.

It is interesting to note that specimen 3A with lower fission heat generation rates in the fuel rod has higher operating temperatures than any of the other rods studied. This is due to the lower thermal conductivity of the slug-injected matrix. The section of this report dealing with metallographic examination shows that the fuel particles irradiated in the better conducting warm-molded matricies (1E, 1D) survived the irradiation in better condition than the particles irradiated in the slug-injected matrix (3A).

POSTIRRADIATION EXAMINATION AND ANALYSIS OF HRB-3

Disassembly and Visual Examination

The capsule was opened by cutting the ends off and splitting the containment tubes into two halves. We recovered the flux dosimeters and several thermocouples for subsequent examination before unloading the fuel rod specimens. The column of specimens was unloaded successfully through the lower end of the graphite sleeve by tapping lightly on the end of the sleeve. All the ORNL specimens were removed intact. The molded specimens were in excellent condition, as typified in Fig. 20 by the appearance of specimens 1E and 1F, which had the highest exposure. The surface cracking that was evident before irradiation did not become more severe, and no chipping or loss of material was seen at the edges. The three slug-injected rods were also in good condition, although specimens 3A and 3B

---

[8] F. J. Homan, *Thermal Analysis of HTGR Fuel Experiments Conducted in the HFIR Removable Beryllium Facility*, (in preparation).

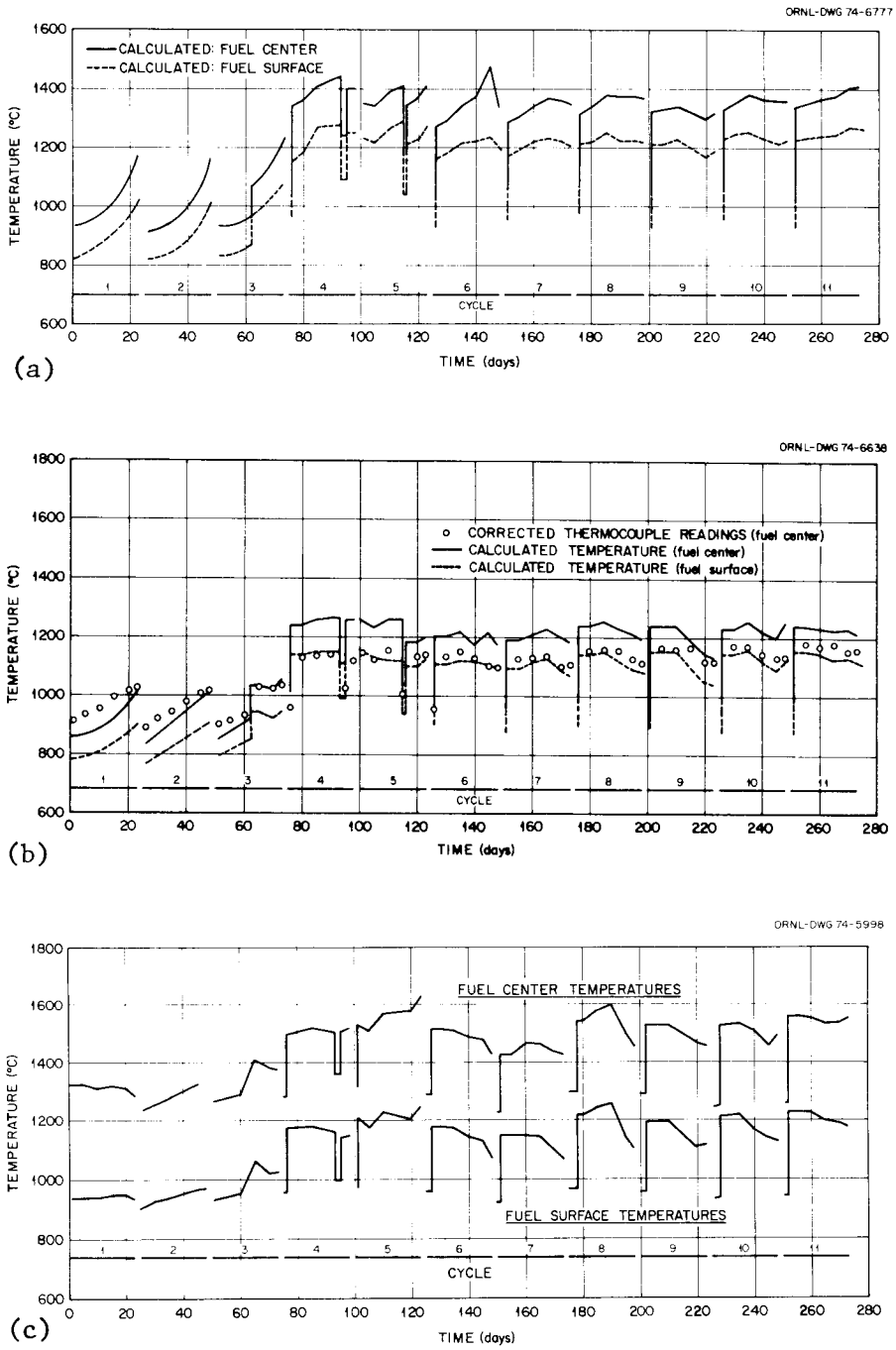

Fig. 19. Fuel Surface and Center Temperatures for HRB-3 Specimens, (a) 1D, (b) 1F, (c) 3A.

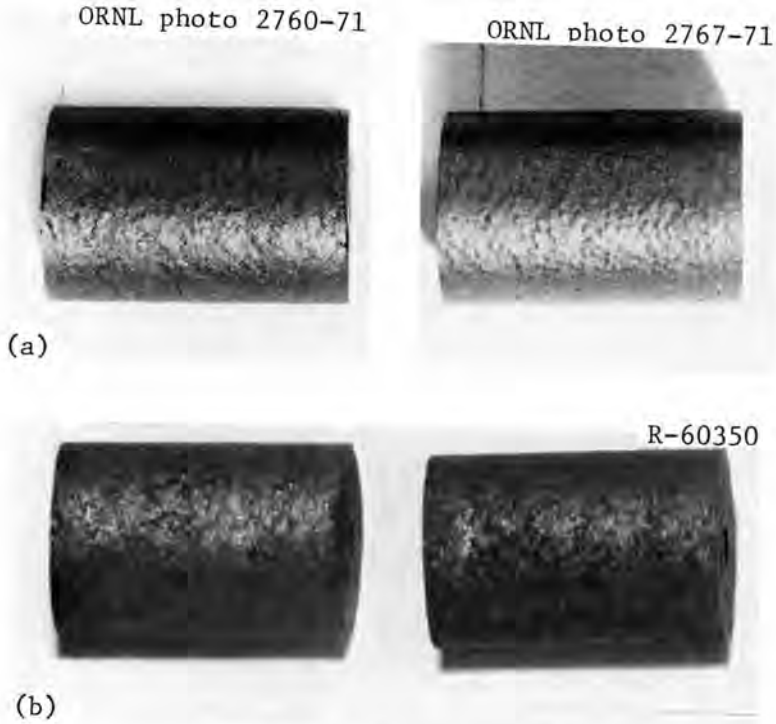

Fig. 20. Appearance of Molded Specimens 1E (left) and 1F (a) Before and (b) After Irradiation.

exhibited some chipping and loss of material due to greater shrinkage associated with the matrix cap. This effect is shown for specimen 3B in Fig. 21, which also illustrates that the remainder of the rod was in excellent condition.

Stereoscopic examination of all specimens confirmed these observations, indicating negligible loss of material from the edges of molded specimens. During stereo examination we observed a few broken coatings on particles at or near the surface of the molded and slug-injected bonded rods, but we could not identify the type of particle that broke. Figure 22 shows a few such broken particles on the surface of one end of specimen 3A.

Dimensional and Weight Changes

After visual examination was completed all ORNL specimens were weighed and measured. Diameters were measured at six positions on the slug-injected specimens 3A, 3B, and 3C and at four positions on the shorter warm-molded specimens. Specimen 3A broke before length measurements could be completed. Average dimensions were then used to calculate shrinkage values, which are compiled in Table 7 along with the calculated fluence. In this table specimens are arranged in order of decreasing fluence. Shrinkage data for the two types of molded specimens are also plotted in Fig. 23 as a function of the fast neutron fluence in order to emphasize effects of exposure.

ORNL photo 2757-71 R-60353

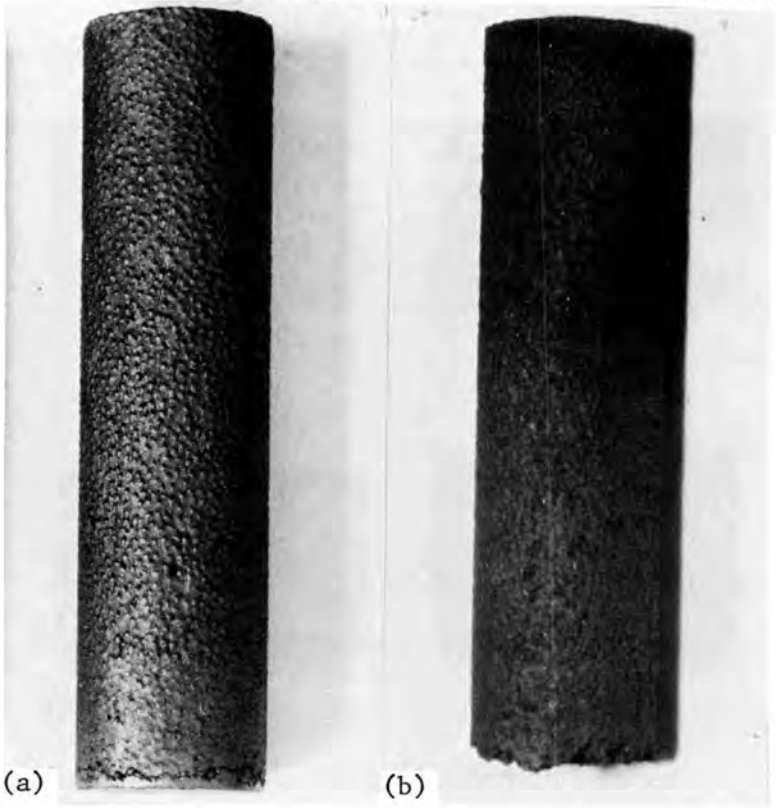

Fig. 21. Appearance of Specimen 3B (a) Before and (b) After Irradiation. Note that the matrix cap crumbled and was lost.

R-60354

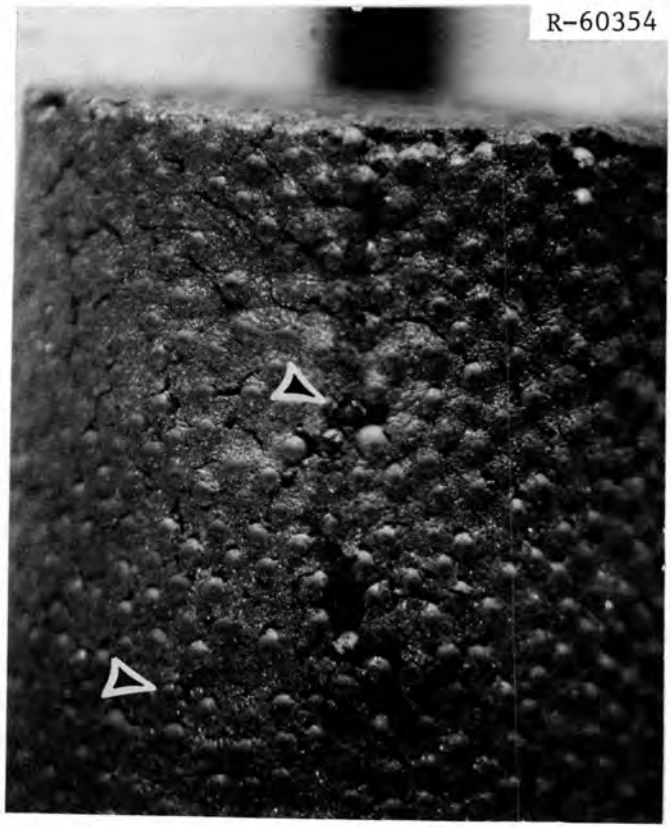

Fig. 22. Surface of Specimen 3A from Capsule HRB-3 Showing Broken Coatings on a Few Particles.

Table 7. Dimensional Changes of Fuel Rod Specimens in HRB-3 Experiment

Specimen[a]	Calculated Fast Fluence, >0.18 MeV (neutrons/cm^2)	Particle Volume Loading (%)	Shrinkage, %	
			Diameter	Length
1E	1.03×10^{22}	32.5	1.49	0.67
1C	0.93	32.5	1.64	0.72
1A	0.80	32.7	1.56	1.55
5A	0.66	32.7	1.78	1.03
6A	0.50	32.7	1.84	1.31
1F	1.07	41.6	1.47	0.69
1D	0.98	41.6	1.58	0.96
1B	0.87	41.6	1.45	1.13
5B	0.58	41.6	1.62	1.25
6B	0.43	41.6	1.64	1.27
3A	1.1	59.7	1.81	b
3B	1.03	59.4	1.83	3.05[c]
3C	0.89	59.5	1.75	1.47

[a]Specimen series 1 consisted of molded rods with central thermocouple holes, series 5 and 6 were solid molded rods, and series 3 was 2-in.-long slug-injected rods.

[b]Specimen 3A was broken during diameter measurement.

[c]Specimen 3B crumbled somewhat at top because of shrinkage associated with matrix cap.

The behavior of the molded specimens was not isotropic. The specimens underwent rapid shrinkage to some minimum dimensions at a low exposure, after which swelling initiated and was more pronounced in the axial direction. The dimensional stability of these molded rods is controlled by the properties of the matrix since the particle coatings are not in contact. Some anisotropy would be expected to develop in the matrix by preferred orientation of the filler materials during compacting. Therefore, behavior of molded specimens is not directly comparable to that of other types of specimens. However, their dimensional stability and performance in the experiment were quite satisfactory.

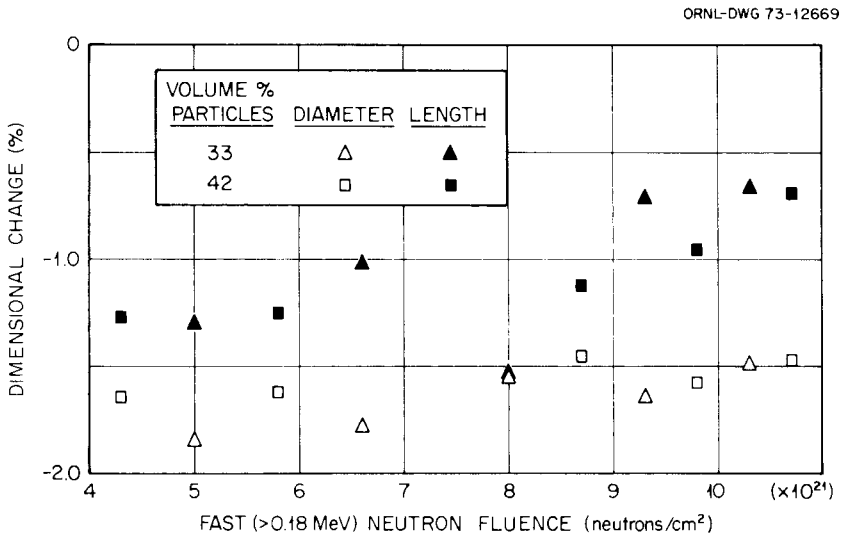

Fig. 23. Effect of Fast Neutron Exposure on Shrinkage of Molded Fuel Rods in Capsule HRB-3.

On the other hand, the shrinkage of the slug-injected specimens was low and isotropic, as would be expected for a blend of particles having high-density outer coatings. For the actual blend of Triso- and Biso-coated inert and fuel particles used in the slug-injected rods, one can calculate a maximum shrinkage of 1.6% as compared with actual values of approximately 1.8%. Shrinkage such as this is quite satisfactory.

Fuel rod dimensional change data from the HRB-3 experiment are compared with data from other experiments in Fig. 24. The solid curve has been described[9] and represents the calculated shrinkage for a slug-injected fuel rod composed of Triso particles having an outer pyrolytic carbon coating with density of 1.85 g/cm^3. The SiC layer of Triso particles provides an unyielding substrate, so only the irradiation-induced densification of the outer layer contributes to the dimensional changes of these rods. The data from the slug-injected rods irradiated in HRB-3 agrees quite well with the solid curve in Fig. 24, in spite of the presence of Biso fertile particles with Triso fissile and inert particles. The data from the HRB-3 warm-molded rods agree well also, but, as was mentioned earlier, these rods appear to be swelling slightly at higher exposure. Data from the ORNL specimens irradiated in P13N are also plotted in Fig. 24. These rods shrank somewhat more than the HRB-3 rods, which were made with the same types of particles. This is probably due to the absence of Triso-coated inert particles in the P13N specimens.

---

[9]J. H. Coobs, J. L. Scott, B. H. Montgomery, J M Robbins, C. B. Pollock, and J. A. Conlin, *Irradiation Performance in HFIR Experiment HRB-2 of HTGR Fuel Sticks Bonded with Reference and Advanced Matrix Materials*, ORNL-TM-3988 (January 1973).

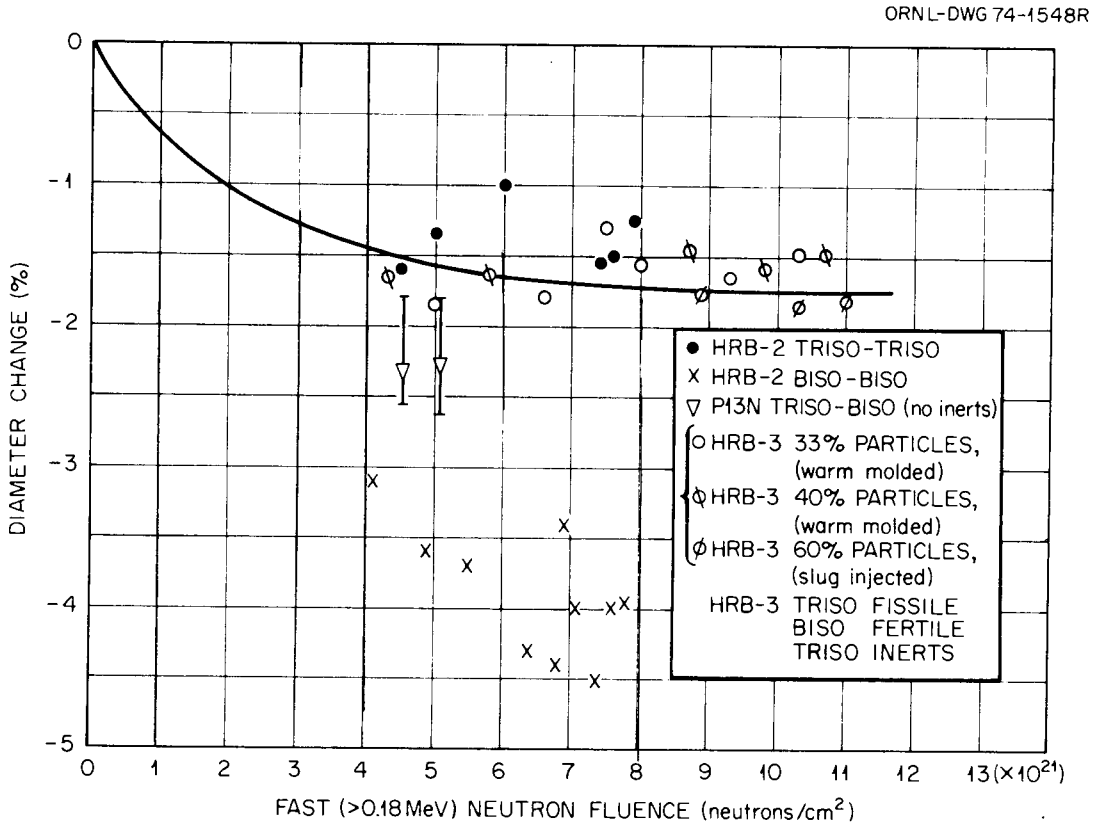

Fig. 24. Variation of Diameter with Fluence in ORNL-Irradiated HTGR Fuel Rods.

Metallographic Examination

Three samples were selected for examination by metallographic techniques. Specimens 1D and 1E were prepared so as to view a longitudinal section, while a cross section near the midplane (broken surface) of specimen 3A was polished for examination. The two GAC specimens were shipped to San Diego, and all other specimens were transferred to dry storage.

Specimen 1D

A polished section of specimen 1D confirmed that the dense matrix of molded specimens was relatively unaffected by the irradiation. Cracks that existed before irradiation grew wider and more noticeable, but no crumbling or spalling of material occurred. The appearance of the dense matrix is illustrated in cross section in Fig. 25. Note that the blocky filler particles of graphite are easily distinguished and that no evidence of coating-matrix interactions was observed.

A portion of the rhenium foil sleeve that protected the central thermocouple adhered to the inner surface of specimen 1D. This sleeve appeared in the polished section, but close examination did not reveal any evidence of a reaction that would explain the adherence.

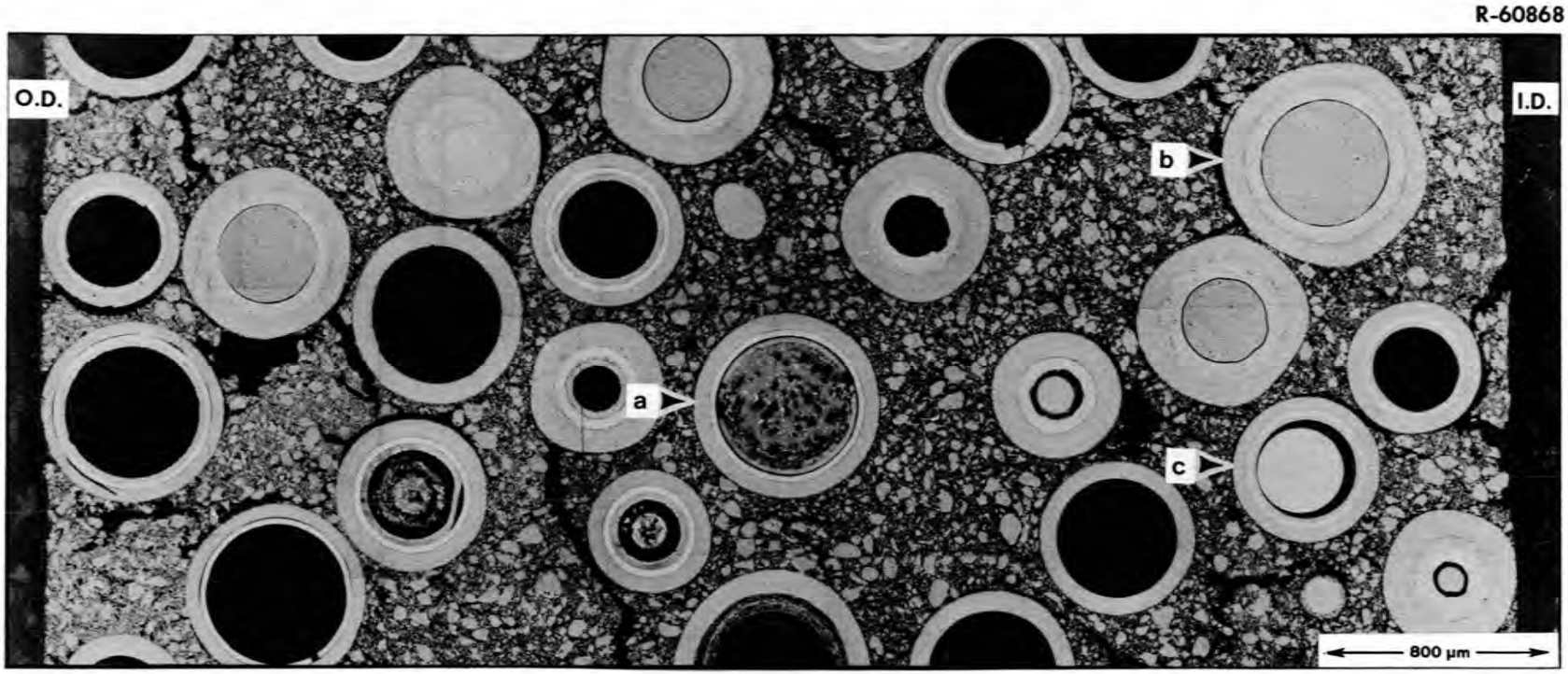

Fig. 25. Cross Section of HRB-3 Molded Specimen 1D Showing (a) Triso-Coated Strong-Acid-Resin Particles, (b) Biso-Coated ThO_2, and (c) Inert Particles.

This specimen contained 42 vol % loading of particles, which consisted of Triso-coated fissile and inert particles and Biso-coated fertile and inert particles. Coating integrity and performance of the particles were adequate to the extent that could be established by examining a small number of particles in one polished section. The Triso-coated fissile particles derived from strong-acid resin exhibited a variety of kernel structures and some attack on the inner isotropic coating and SiC layers of some particles. This phenomenon is evident in Fig. 25 and does not seem to be influenced by radial position in the fuel rod or temperature gradients within the particles. More detailed discussion of this behavior is presented later.

Specimen 1E

A longitudinal polished section of specimen 1E also indicated that the dense matrix of molded rods performed well. This specimen had a lower volume loading (32.5%) than 1D and a slightly higher matrix density, but the appearance of the matrix was quite similar. The same variety of kernel structures in the Triso-coated fissile particles was also observed. The only unusual feature in the entire section was the apparent initiation of kernel migration (amoeba effect) in one Biso-coated ThO_2 particle. The thin deposit of highly oriented carbon, shown in Fig. 26, is located in the direction of the outer surface of the fuel rod, as expected. However, no actual movement or migration of this fuel kernel is detectable. This particle was located about 2 mm from the outer surface of the rod.

Specimen 3A

The cross section near the middle of specimen 3A emphasizes the contrast between the matrix of slug-injected and molded fuel rods. The radial section in Fig. 27 shows between particles the large pores and clumps of matrix material that are characteristic of slug-injected rods. Some kernels and matrix material were lost in metallographic preparation, but this structure is fairly typical of rods with a low-density matrix ($\sim$0.6 g/cm^3).

The microstructure of the matrix material near the rod surface is shown in some detail in Fig. 28. The large amount of microporosity and the clear resolution of the flake-graphite filler material are quite evident. The residual coke from carbonization of the pitch, which binds the filler particles together in the matrix, is present in most of the structure as a thin film on or between particles of graphite filler. The difference between coke and graphite filler is clearly distinquished in the polarized-light micrograph [Fig. 27 (b)]. A clump of matrix material near the center of the rod showed a larger fraction of pitch coke, but the porosity and structure are similar to that at the surface. Such structures are preferred for fuel rod stability and lack of coating-matrix interactions, but the low density and discontinuous nature of the matrix contributes little to heat conduction within the fuel rod.

The most significant observation on particle behavior in specimen 3A was the measurable migration of six Biso-coated ThO_2 particles; three were observed in each of two polished sections prepared on this specimen.

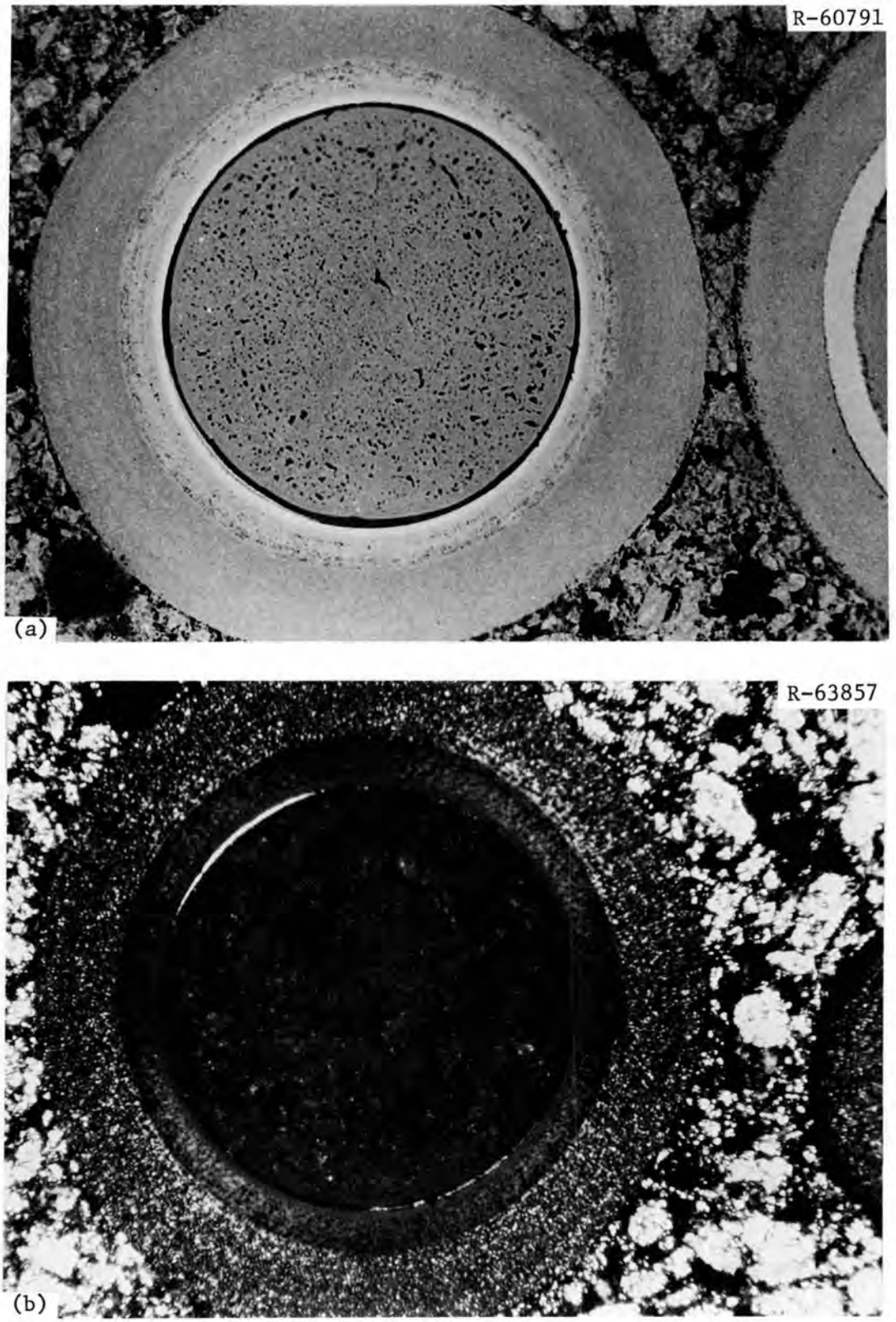

Fig. 26. Cross Section of Biso-Coated ThO_2 Particle in Specimen 1E from Capsule HRB-3. Note the thin deposit of highly oriented carbon, which is located on the side away from the highest temperature. 200×. (a) Bright field, as polished. (b) Polarized light.

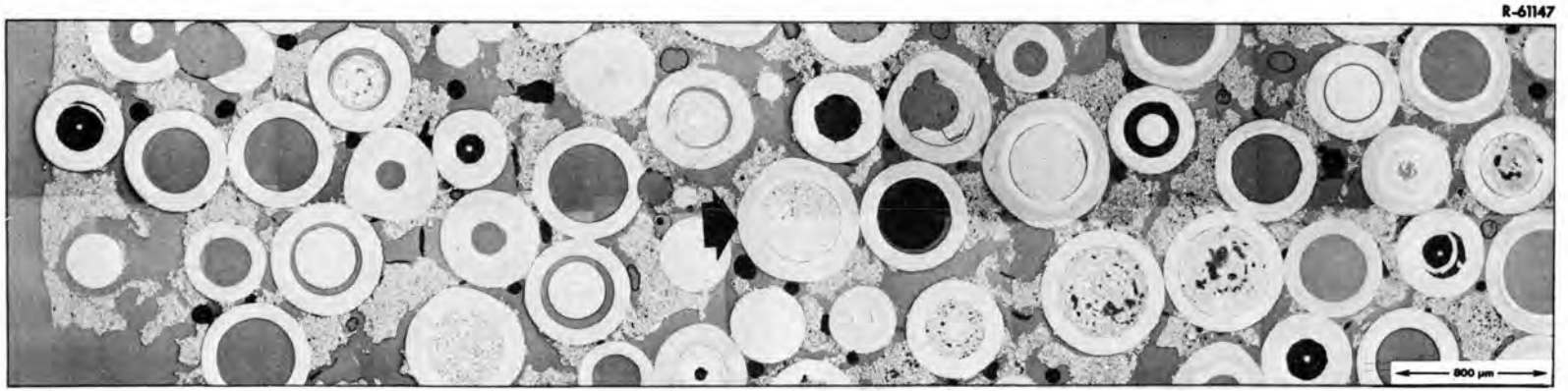

Fig. 27. Cross Section of Slug-Injection-Bonded Specimen 3A from Capsule HRB Biso-coated ThO_2, Triso-coated resin-derived fissile, and inert particles bonded w Fort St. Vrain matrix material. Arrow indicates ThO_2 particle with slight amoeba

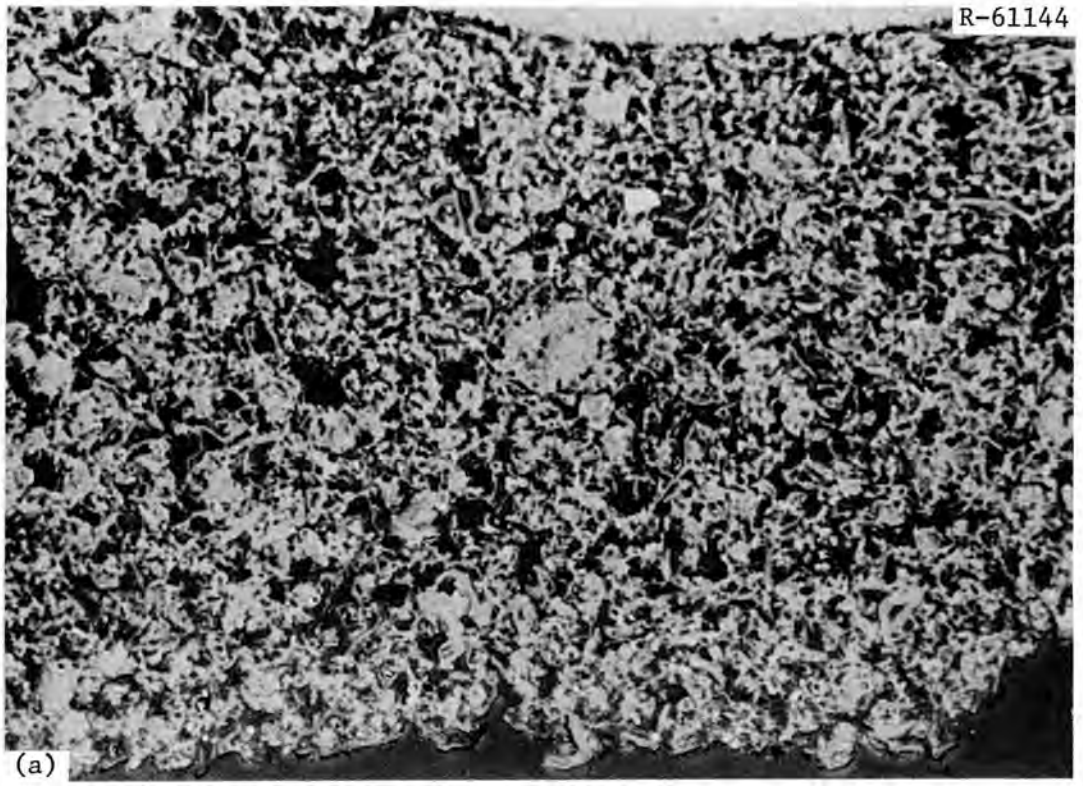

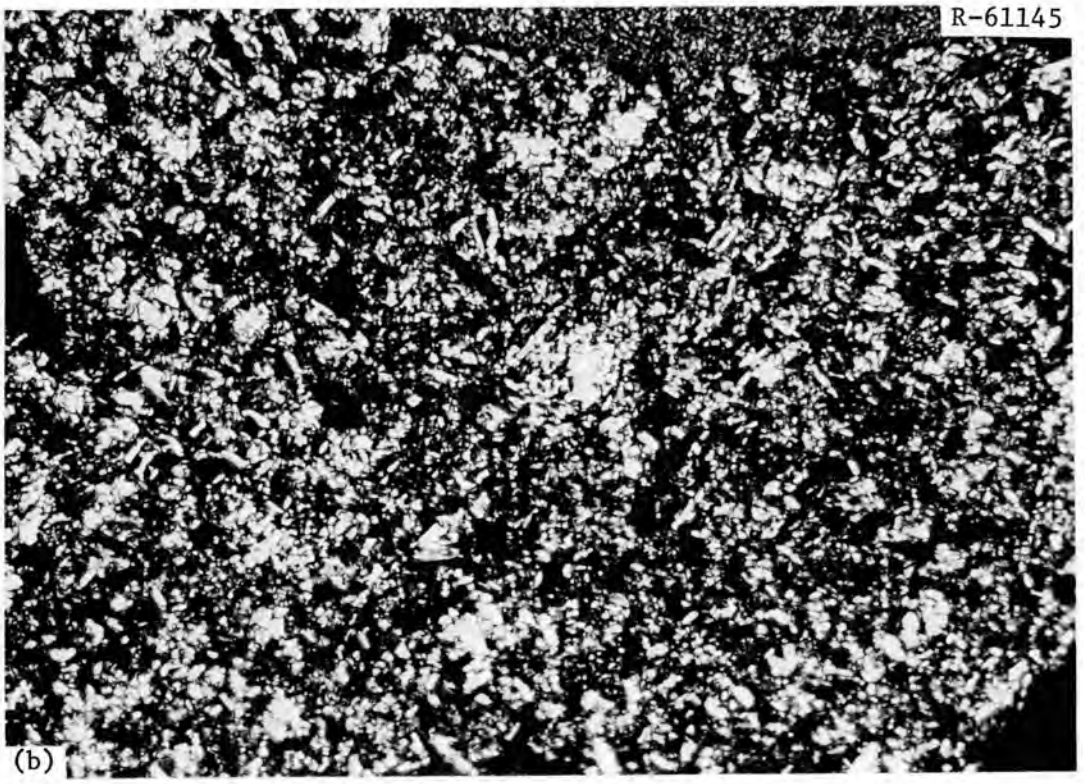

Fig. 28. Structure of Slug-Injected Matrix Material near Surface of Specimen 3A from Capsule HRB-3. As polished, 500×. (a) Bright field. (b) Polarized light.

One such particle is shown near the middle of Fig. 27, at a position about 4 mm from the outer surface of the rod. The particle that exhibited the greatest amount of migration is shown in Fig. 29. Close examination of the bright-field and polarized-light micrographs indicates that the highly oriented carbon was deposited in at least four separate stages and that the last stage represents a large fraction of the total deposited. This implies that temperature gradients may have been greater during late stages of capsule operation or that the migration is strongly affected by exposure and burnup of the fuel.

The observation of kernel migration in the ThO_2 particles is significant, because this was the first ORNL irradiation experiment in which such migration was seen. Thoria is the most stable of the dense-kernel fuels. A complete tabulation of existing information on relative thermal stabilities can be found in other reports.[10-13]

Fissile Particle Behavior

In all three specimens the strong-acid-resin-derived fissile particles exhibited various structures and some instances of attack on inner carbon and SiC coating layers. A buffer layer was not included in the design of these particles. Some typical micrographs are shown in Figs. 30 and 31. Figure 30 illustrates the banded structure observed in many of the fissile particles. This segregation of phases within the fuel kernel did not adversely affect performance except as it may have contributed to the attack on the inner LTI and SiC barrier layers. The presence of dense deposits at the inner surface of the SiC layer and the initiation of attack on this layer are evident in both particles that have intact inner LTI coatings. The particle shown in Fig. 30, from molded specimen 1D, exhibits less transformation and less attack on the SiC layer, than the particle shown in Fig. 31 (a), but this was generally true of fissile particles in the molded specimens, where maximum fuel temperatures were lower. A more advanced stage of this attack on the SiC layer is shown in Fig. 31(b), in which the inner LTI coating has been breached and significant attack and removal of SiC occurred. This stage was accompanied by formation of the white crystalline deposits within the kernel.

Examination of the fissile particles from the three samples examined metallographically showed that no gross coating failures or breach of the

---

[10] R. A. Olstad et al., *An Irradiation of Candidate HTGR Fuels in the H-1 and H-2 Capsules*, ORNL-TM-4397 (July 1974).

[11] T. B. Lindemer and H. J. de Nordwall, *An Analysis of Chemical Failure in Coated UO_2 and other Oxide Particles in the High-Temperature Gas-Cooled Reactor*, ORNL-4926 (January 1974).

[12] T. B. Lindemer and R. A. Olstad, *HTGR Fuel Kernel Migration Data for the Th-U-C-O System as of April 1, 1974*, ORNL-TM-4493 (June 1974).

[13] T. D. Gulden, J. L. Scott, and C. Moreau, "Present Thorium-Cycle Concepts and Performance Limitations," pp. 176-200 in *Gas-Cooled Reactors: HTGR and GCFBR*, (Proceedings of ANS Topical Meeting, May 7-10, 1974, Gatlinburg, Tenn), CONF-740501.

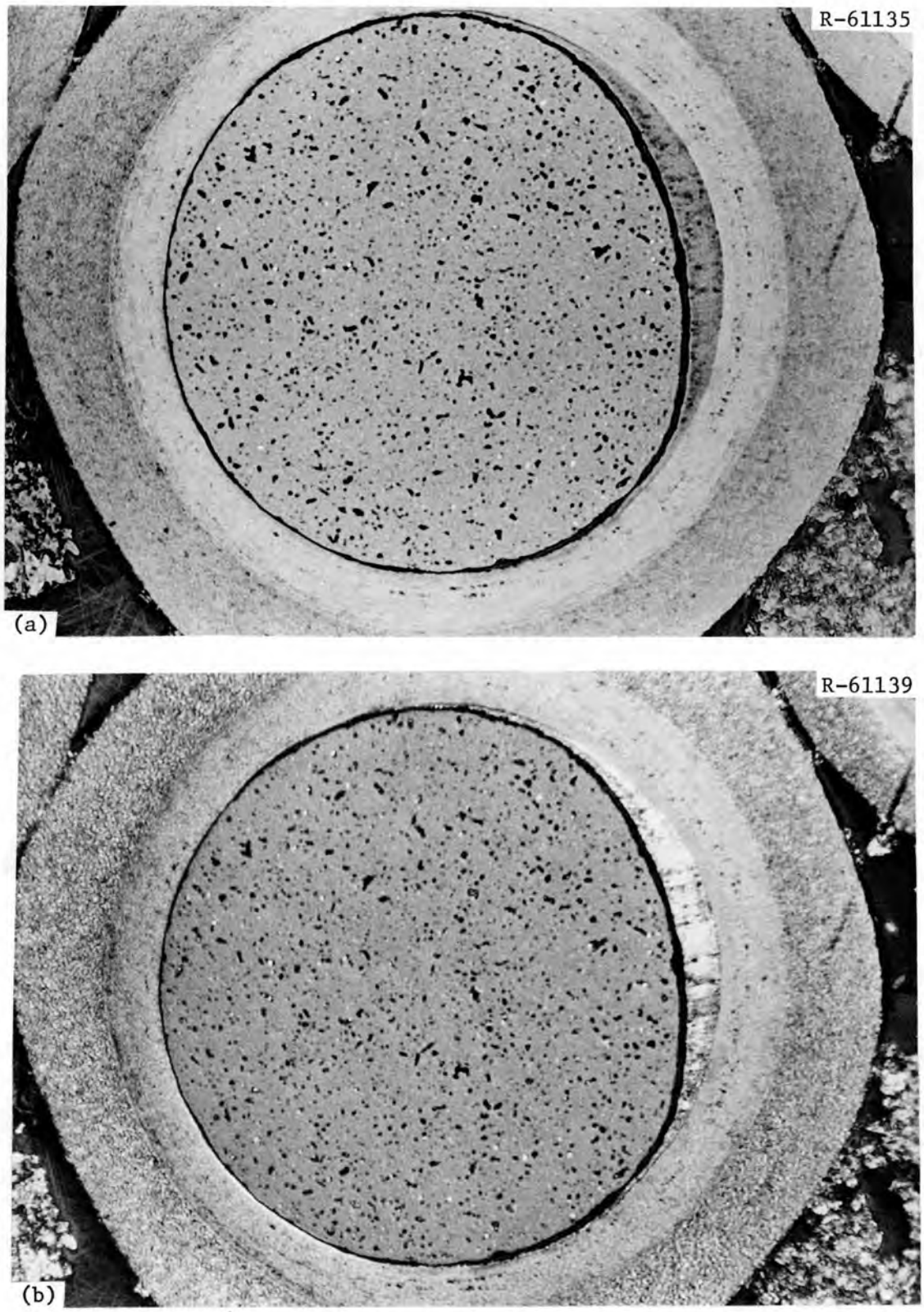

Fig. 29. Polished Section of Biso-Coated ThO_2 Particle Showing Maximum Kernel Migration in Specimen 3A of Capsule HRB-3. As polished, 200×. (a) Bright field. (b) Polarized light.

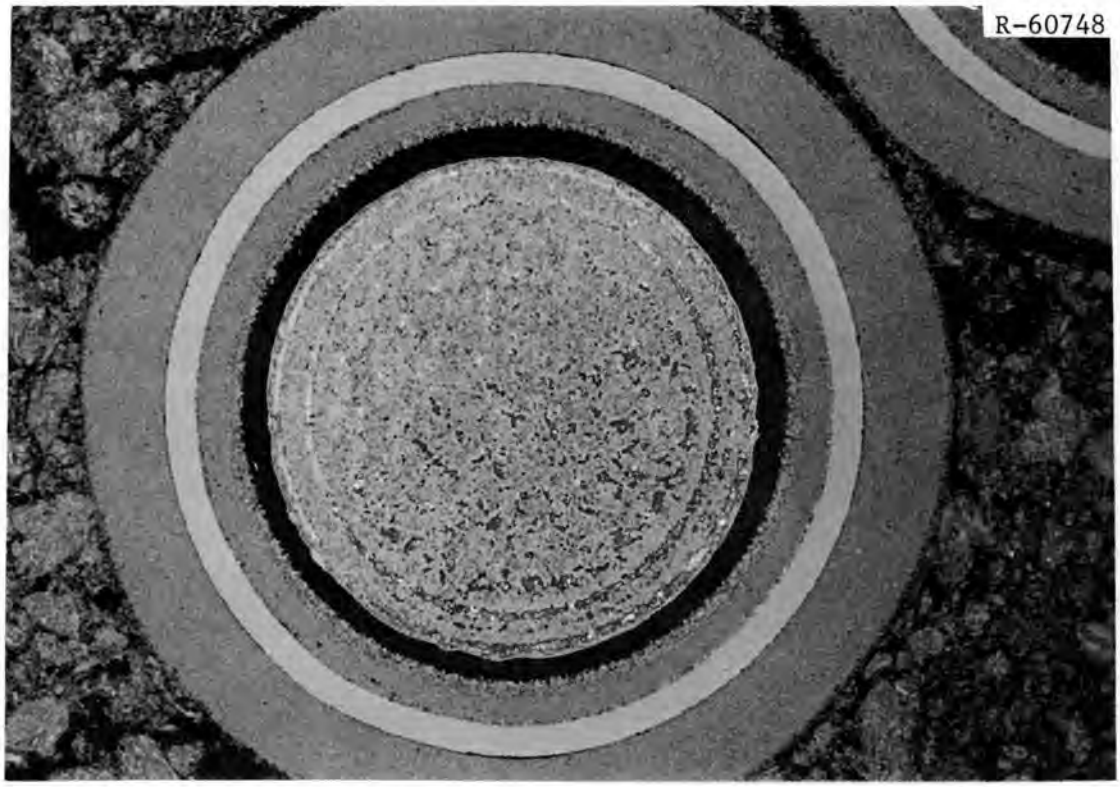

Fig. 30. Triso-Coated Fissile Particle Derived from Strong-Acid Resin and Irradiated in Capsule HRB-3, Specimen 1D. As polished, 200×.

SiC layer occurred. In a number of instances the inner LTI coating failed and some fission product attack of the SiC coating occurred. The fission product attack was much more severe when the inner LTI failed. The cause of the failure of the inner LTI is not discernible from the visual examination and could be either fission recoil damage or a mechanical interaction between kernel and coating. Since many inner LTI coatings did not fail even though they received severe fission recoil exposure, it is more likely that the cause of failure was too good a bond between the inner LTI coating and the kernel, which shrinks rapidly at the onset of irradiation. When kernels separated cleanly from coatings, no inner LTI coating failures were observed. On the basis of these observations we concluded that a thin buffer layer is required on resin kernels to prevent a mechanical interaction with the coating.

No amoeba migration in the resin-derived kernels was observed, even though conditions were severe enough to induce amoeba migration in the ThO_2 kernels. This observation will be discussed later.

ORNL SPECIMENS FROM ETR CAPSULE P13N

Two ORNL slurry-blended, warm molded fuel rod specimens were irradiated in two compartments of a five-compartment instrumented ETR capsule P13N along with 20 other fuel rod specimens fabricated by Gulf General Atomic. This capsule was designed by GGA as a part of their thermal

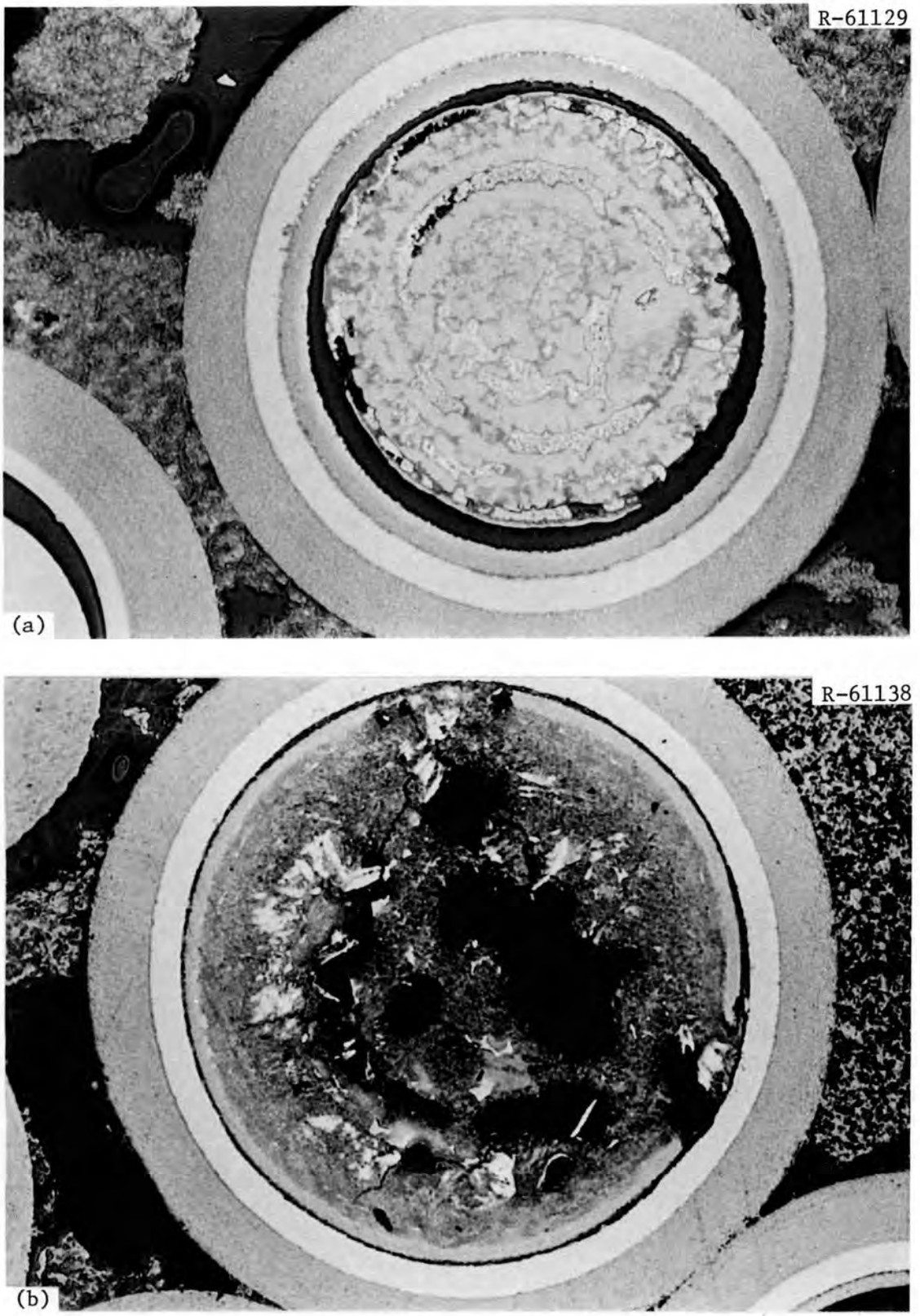

Fig. 31. Triso-Coated Fissile Particles Derived from Strong-Acid Resins and Irradiated in Capsule HRB-3, Specimen 3A. As polished, 200×.

stability tests; their results are reported separately.[14] The irradiation behavior of these specimens is being reported here because they contained the same fuel (strong-acid-resin-derived fissile particles and thoria fertile particles) as the HRB-3 specimens. In fact, the fertile particles are from the same batch and the matrix is also identical to that used in the molded fuel rods in HRB-3. The design of the fissile particles was also the same — no buffer coating was used. The uranium was fully enriched (90.8% ^{235}U) in P13N, but only 7% enriched in HRB-3.

Fabrication

The ORNL P13N specimens contained a nominal 42 vol % loading of Triso-coated, fully enriched strong-acid-resin kernels (OR-1602) and Biso-coated ThO_2 fertile kernels (OR-1562). The characteristics of the coated particles used in the ORNL fuel rods are shown in Tables 8 and 9.

[14] Gulf General Atomic, *HTGR Base Program Quart. Progr. Rep. Aug. 31, 1973*, Gulf GA-A 12725, pp. 190-234.

Table 8. Characteristics of Coated Particles Used in ORNL Bonded Beds for P13N.

Characteristics	Value for Each Batch	
	OR-1602	OR-1562
Fuel Material	UCS	ThO_2
Uranium Content, wt %	13.0	
^{235}U Enrichment, at. %	90.8	
Thorium Content, wt %		51.6
Density of Coated Particle[a] (g/cm^3)	2.10	3.48
Coating Density[b] (g/cm^3):		
Buffer	none	1.2[c]
Inner	1.9[d]	
SiC	3.21 ± 0.001	
Outer	1.94 ± 0.003	1.97 ± 0.007

[a] Measured by mercury porosimetry.

[b] Measured by density gradient column. Average of densities from fragments of 10 and 15 particles ± standard deviation.

[c] Calculated.

[d] Estimated from coating condition.

Table 9. Dimensions of Coated Particles Used in ORNL Bonded Beds for P13N

Measurement	Value,[a] μm			
	Average	Maximum	Minimum	Std Deviation
	Batch OR-1602 (fissile)			
Total particle diameter	661	750	607	32
Kernel diameter	388	499	329	35
Coating thickness				
Inner	25	34	18	4
SiC	19	21	16	1
Outer	92	104	85	4
	Batch OR-1562 (fertile)			
Total particle diameter	660	709	602	33
Kernel diameter	398	431	355	17
Coating thickness				
Buffer	55	69	36	8
Outer	76	90	64	6

[a]Results from measurements taken on 25 particles.

The same matrix and Biso-coated ThO_2 fertile kernels from Batch OR-1562 were used also in fuel rods irradiated in HRB-3. Some of the characteristics of the fuel rods used in capsule P13N are given in Table 10. The rods were fabricated by the following sequence:

1. coated particles heat-treated at 1800°C for 30 min;

Table 10. Characteristics of Warm-Molded Fuel Rods Irradiated in Capsule P13N[a]

Fuel Rod[b]	Particle Loading (%)	Fuel Content, g			Preirradiated Fission-Gas Release,[c] *R/B*
		U	^{235}U	Th	
1D-1	42.5	0.0665	0.0604	1.3132	3.2×10^{-6}
3A-1	42.6	0.0522	0.0474	1.4040	4.0

[a]Matrix Composition: 31.5 wt % Ashland Grade 240 pitch, 53.5 wt % GCL 1074 graphite powder, and 15.0 wt % Thermax. Density: 1.43 g/cm^3.

[b]Fuel rods were nominally 0.49 in. diam × 0.73 in. long.

[c]*R/B* for ^{85m}Kr at 1400°C.

2. matrix and particles slurry blended in benzene and acetone, solvents evaporated, and green fuel rods formed at 165°C at 1000 psi;
3. fuel rods carbonized in a bed of flake graphite powder at 1000°C over a 24-hr period;
4. carbonized fuel rods heat-treated in flowing argon at 1800°C for 30 min.

The preirradiation appearance of the fuel rods used in this irradiation test is shown in Fig. 32. The microstructure of fuel rods fabricated along with the irradiation specimens is shown in Figs. 33 through 35. After dimensional inspection the fuel rods were shipped to GGA for incorporation in irradiation capsule P13N.

Irradiation

Capsule P13N was inserted in the ETR January 19, 1972 and completed its scheduled irradiation on January 5, 1973 after 3732 effective full-power hours of operation. The prime irradiation conditions[15] are summarized in Tables 11 and 12. A preliminary thermal analysis indicated that peak

[15]Private communication from D. P. Harmon (GAC) to J. H. Coobs (ORNL) Sept. 26, 1973 and Oct. 5, 1973.

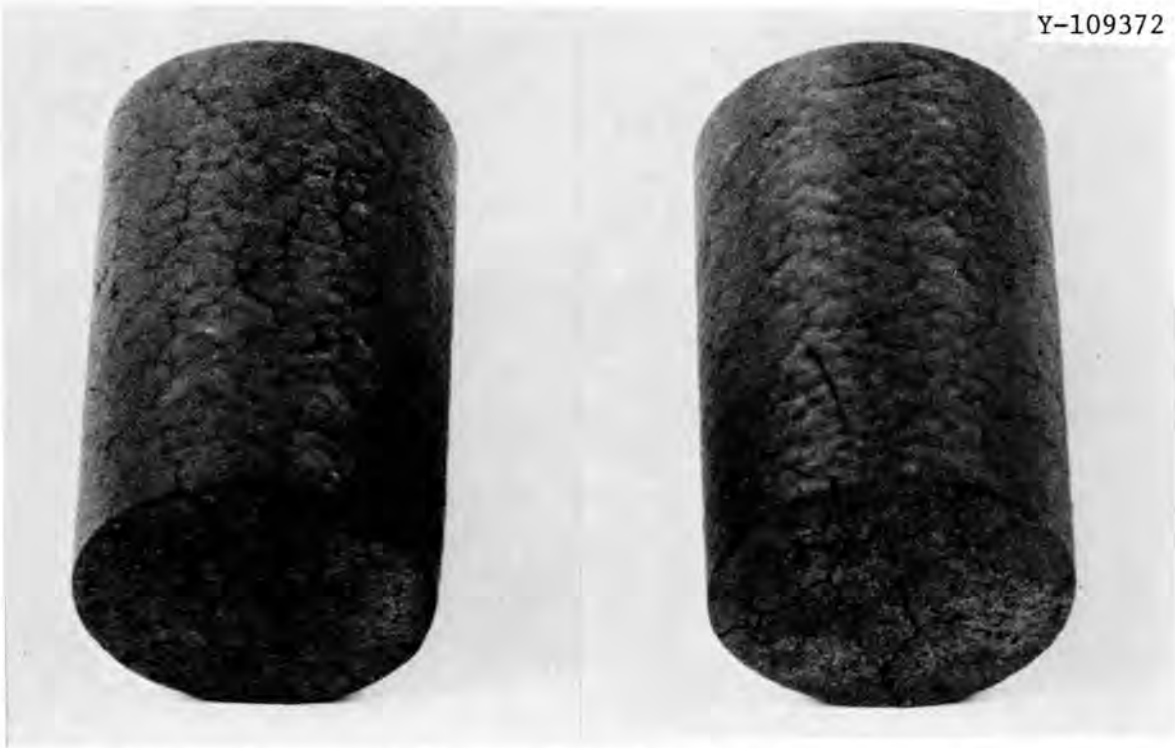

Fig. 32. Appearance of Warm-Molded Fuel Rod Specimens Before Loading into Irradiation Capsule P13N. 3.8× Left: Fuel rod 1A-1. Right: rod 3A-1.

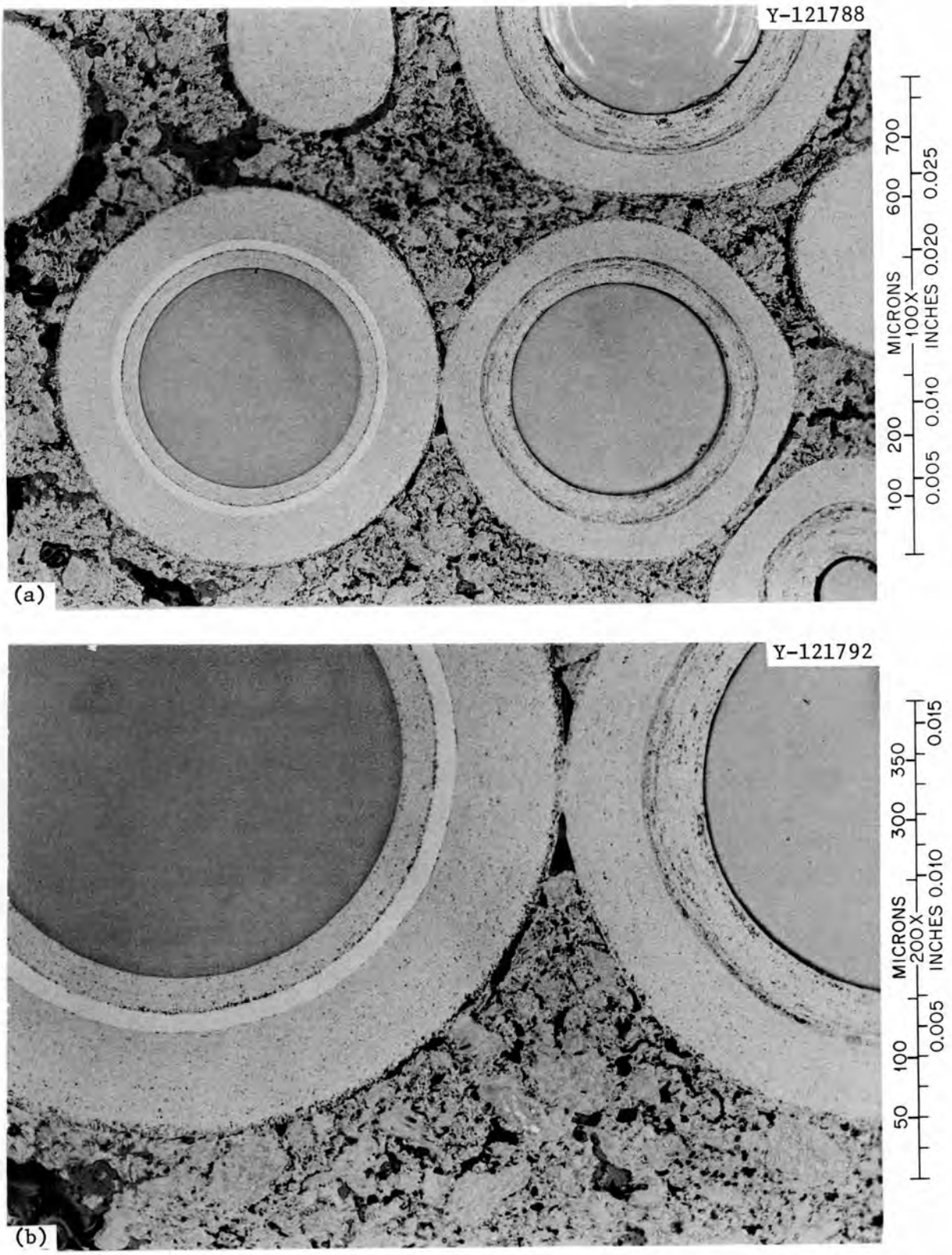

Fig. 33. Microstructural Features of Unirradiated Warm-Molded Fuel Rods. The Strong-Acid-Resin Kernels (UCS) are Triso Coated; the ThO_2 Kernels are Biso Coated.

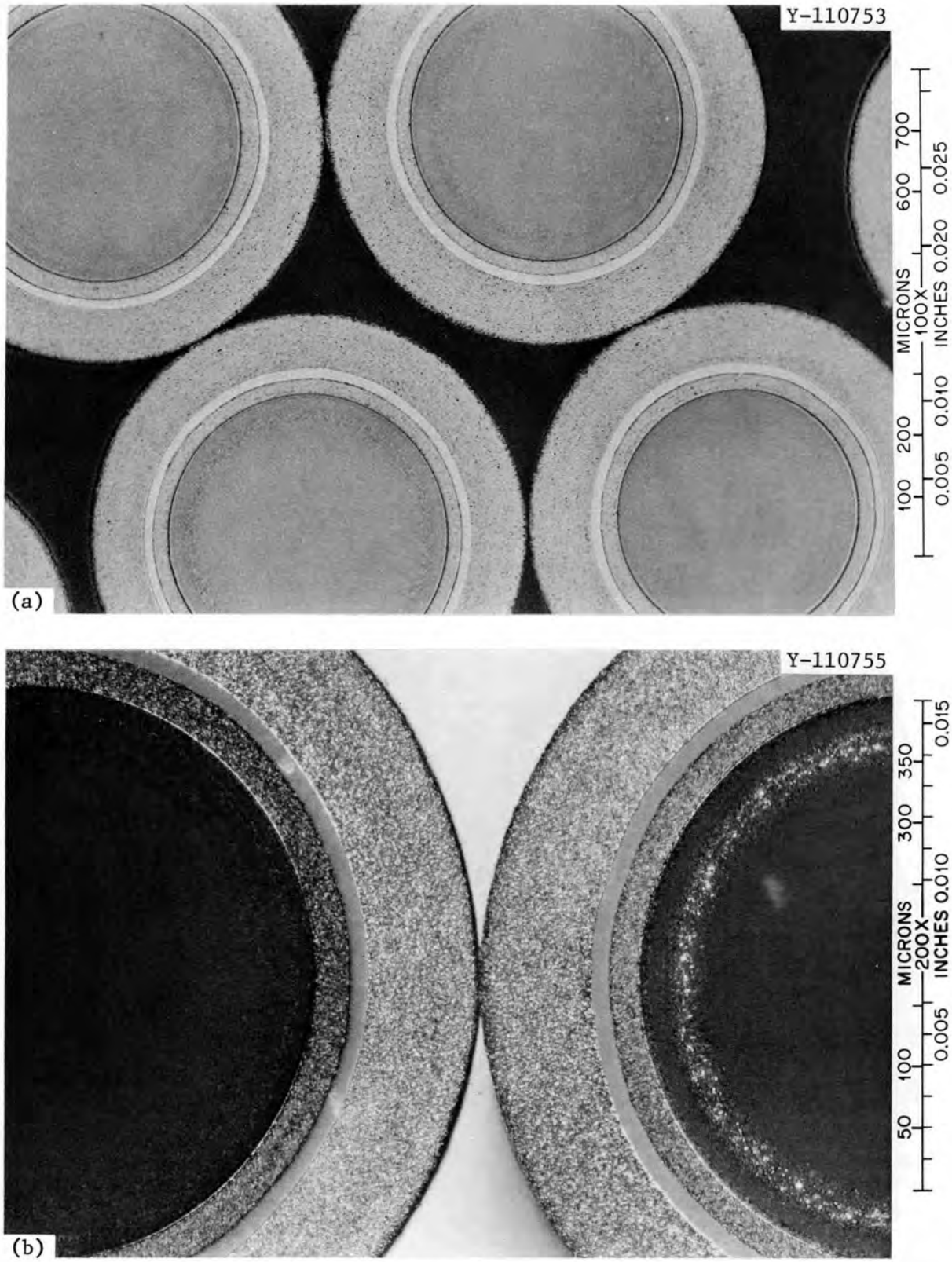

Fig. 34. Microstructure of Triso-Coated Strong-Acid-Resin Kernels Before Incorporation into Fuel Rods. (a) Bright field; (b) Polarized light.

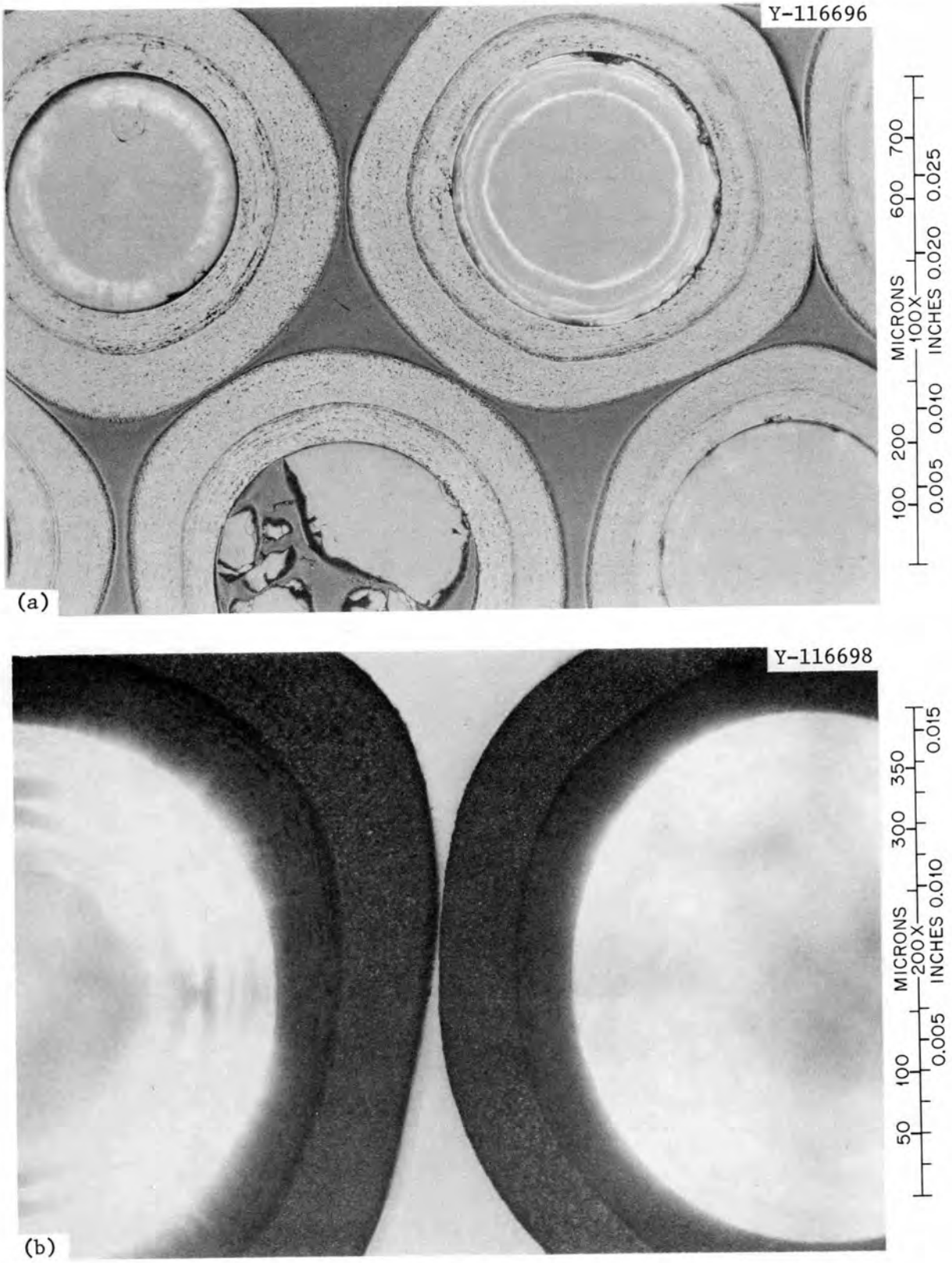

Fig. 35. Microstructure of Biso-Coated Sol-Gel ThO_2 Kernels Before Incorporation into Fuel Rods. The edges of the ThO_2 microspheres were chipped during metallographic preparation. (a) Bright Field; (b) Polarized Light.

Table 11. Irradiation History for ORNL Fuel Rods in Capsule P13N

Condition	Value for Each Fuel Rod	
	1D-1	3A-1
Temperature, °C		
Center line (integrated average)	1415	1480
Surface, beginning of life	985	1110
Surface, end of life	1230	1220
Effective full-power hours	3732	3732
Burnup, % FIMA		
fissile	65	66
fertile	1.8	2.0
Fast (>0.18 MeV) fluence, neutrons/cm^2	4.6×10^{21}	5.1×10^{21}
Fission gas release (R/B ^{85m}Kr)		
preirradiation at 1400°C	3.2×10^{-6}	4.0×10^{-6}
postirradiation at 1100°C[a]	1.4×10^{-4}	2.6×10^{-5}

[a]Not corrected for steady state.

Table 12. Thermal History of ORNL Fuel Rods in Capsule P13N

Rod 1D-1			Rod 3A-1		
Calculated Fuel Rod Central Temperature (°C)	Time in Temperature Range		Calculated Fuel Rod Central Temperature (°C)	Time in Temperature Range	
	(hr)	(%)		(hr)	(%)
895	96	2.6	1010	40	1.1
963	96	2.6	1088	128	3.4
1031	168	4.5	1165	176	4.7
1100	216	5.7	1243	160	4.3
1168	48	1.3	1321	928	24.6
1236	40	1.1	1399	576	15.3
1304	64	1.7	1477	544	14.4
1372	256	6.8	1554	224	5.9
1440	1664	44.2	1632	440	11.7
1509	1120	29.7	1710	552	14.7
1576			1788		

center-line temperatures may have exceeded the listed integrated average temperatures by as much as 300°C for a significant period of time as reflected in Table 12. A detailed thermal analysis will be performed later by GAC.[16] The temperatures tabulated in Table 12 can be compared with HRB-3 specimen temperatures in Fig. 19, p. 24.

Postirradiation Examination

Physical Examination

The capsule was disassembled and the ORNL fuel rod specimens were examined in the GAC hot-cell facility. The appearance of the specimens was excellent, with no evidence of debonding. One broken coating was noted on the surface of specimen 3A-1, but no other damage was evident. Dimensional inspection of the specimens showed an average diametral shrinkage of about 2.4%, and the decrease in length averaged about 1.8%, as shown in Table 13. The fuel rod specimens were shipped to the

[16]Personal communication with D. P. Harmon, GAC.

Table 13. Dimensions of ORNL Fuel Rods Irradiated in Capsule P13N

Fuel Rod	Orientation[a] (Deg)		Dimensions, in		Decrease	
			Preirradiation	Postirradiation	(in.)	(%)
1D-1 (44B)	T	0	0.4902	0.4788	0.0114	2.32
	T	90	0.4907	0.4799	0.0108	2.20
	M	0	0.4916	0.4805	0.0111	2.26
	M	90	0.4918	0.4798	0.0120	2.44
	B	0	0.4905	0.4773	0.0132	2.69
	B	90	0.4905	0.4779	0.0126	2.57
	L	0	0.7345			
	L	90	0.7342			
	L	C	0.7350	0.7219	0.0131	1.78
3A-1 (45B)	T	0	0.4904	0.4775	0.0129	2.63
	T	90	0.4897	0.4786	0.0111	2.27
	M	0	0.4916	0.4789	0.0127	2.58
	M	90	0.4914	0.4789	0.0125	2.54
	B	0	0.4909	0.4788	0.0121	2.46
	B	90	0.4904	0.4788	0.0116	2.36
	L	0	0.7354	0.7219	0.0135	1.84
	L	90	0.7344	0.7212	0.0132	1.80
	L	C	0.7350	0.7212	0.0138	1.88

[a]Diameter measured at T = top, M = middle, and B = bottom of fuel rod. L = length.

High-Radiation Level Examination Laboratory (HRLEL) at ORNL for a more detailed examination. A stereo examination of the two specimens was made and compared with photomacrographs supplied by GAC. No damage was evident that could be attributed to shipping. The appearance of the two specimens is shown in Fig. 36. However, a notable change was seen in the appearance of one of the specimens; a white crystalline material had fromed in the central region of one end of specimen 1D-1. The appearance of this fuel rod specimen while in the GAC hot cells and the ORNL hot cells is compared in Fig. 37. A material similar in appearance has been observed in irradiated bulk-oxide fuels that have been exposed to air; it was tentatively identified as an alkali-metal hydrous carbonate.[17] A gamma spectral analysis of a small sample of the foreign material on the fuel rod specimen confirmed that it contained primarily the fission products cesium, cerium, barium, and lanthanum.

Both the fuel rod specimens were intentionally broken at about mid-length; one-half of each specimen was submitted for metallographic preparation, and the remaining halves were stored for possible later disintegration studies. Stereo examination of the fracture surface revealed no evidence of broken particles.

---

[17]D. R. Cuneo and R. B. Fitts, *GCR Program Semiannu. Progr. Rep. Sept. 30, 1969,* ORNL-4508, pp. 74–75.

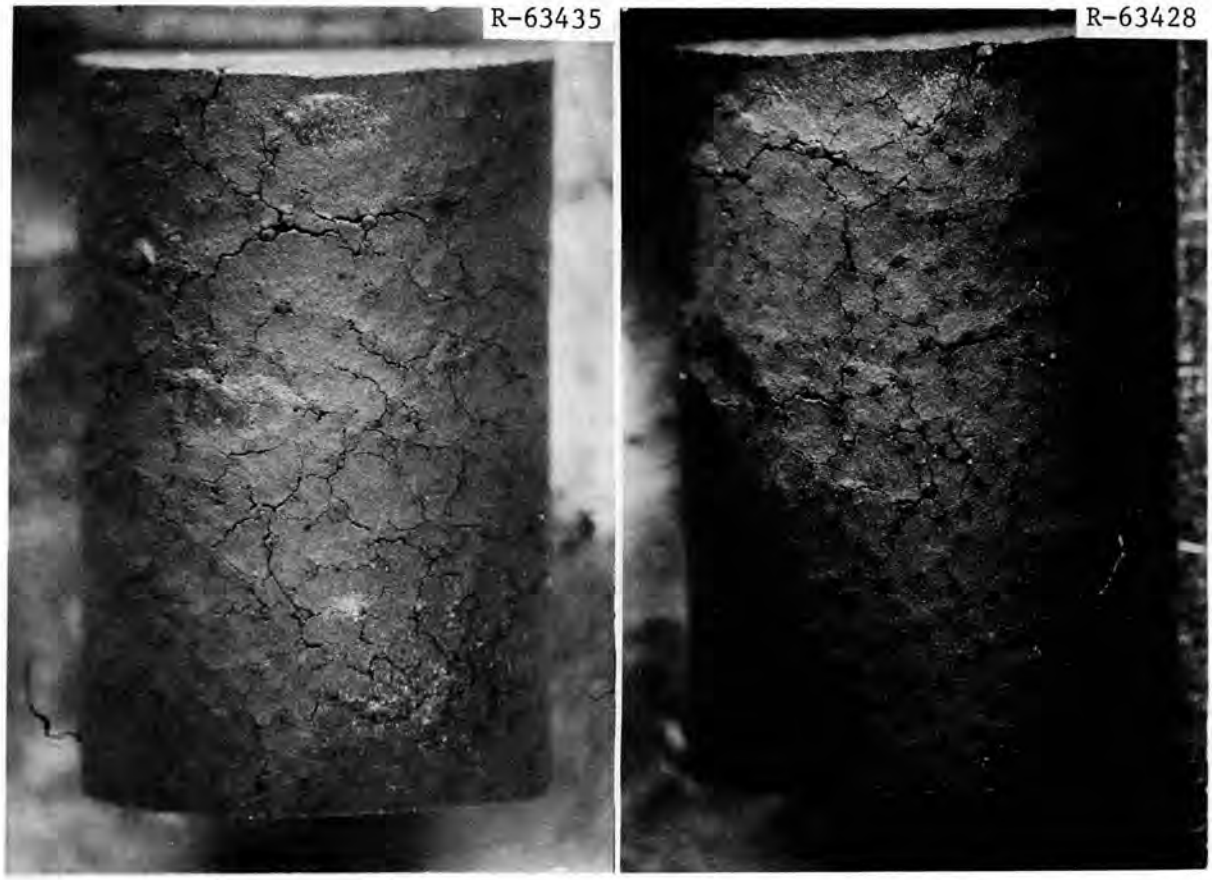

Fig. 36. Appearance of Irradiated Fuel Rods After Removal from Irradiation Capsule P13N. 5×. Left: Fuel Rod 1D-1. Right: Fuel Rod 3A-1.

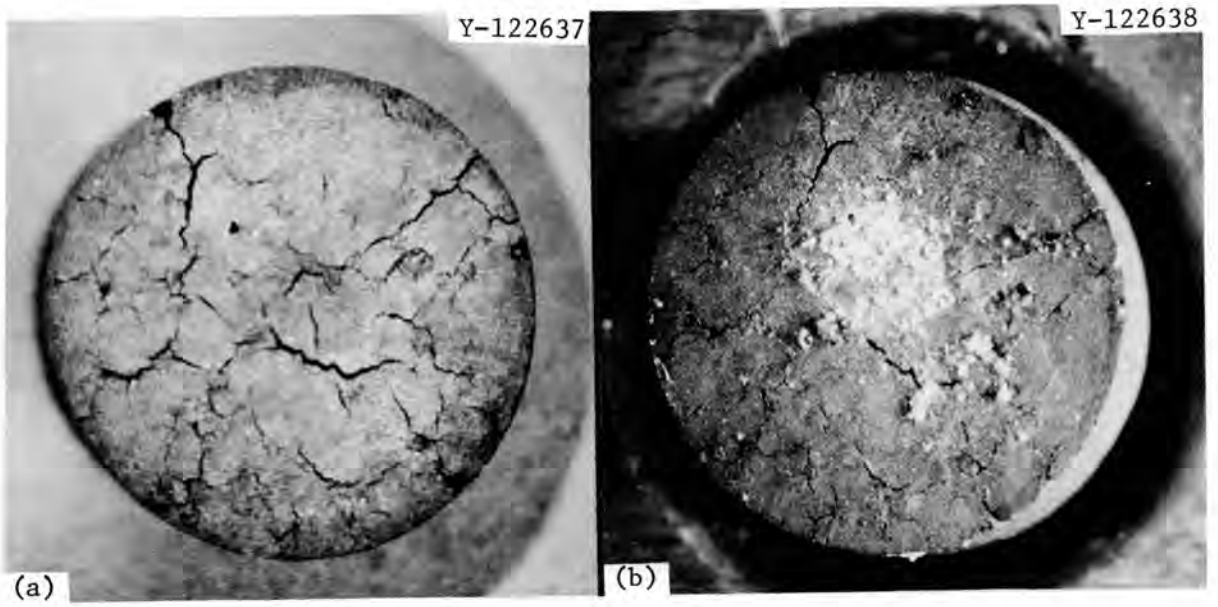

Fig. 37. Appearance of Fuel Rod Specimen 1D-1. 5×. (a) Shortly after removal from the irradiation capsule at GAC and (b) after shipment to the ORNL hot cells.

Metallographic Examination

The Metallographic specimen taken from fuel rod 1D-1 was mounted for a longitudinal section, and a transverse section was prepared at about the midlength of fuel rod specimen 3A-1. The macroscopic appearance of these two metallographic sections is shown in Figs. 38 and 39. Metallographic examination of these two specimens yielded similar results. The plane of polish through each specimen exposed 34 Triso-coated strong-acid-resin (SAR) particles. A significant number of these SAR kernels exhibited the "amoeba" effect (50% in specimen 1D-1 and 41% in specimen 3A-1). Close examination of the SAR particles that exhibited the "amoeba" effect revealed that, typical of this effect in other coated particle systems, the migration was toward the hot side of the particle. In fuel rod 1D-1, 27% of the SiC coatings had failed and 38% in fuel rod 3A-1 from the "amoeba" effect. Examples of the appearance of the SAR particles in both sections are shown in Fig. 40. As can be seen in the Fig. 40, the kernel destroyed the inner LTI coating, dissolved the SiC on the hot side, and appears to have rejected silicon on the cold side of the particle. The "amoeba" migration was more pronounced in the peripheral region of the fuel rods, but was observed in particles near midradius, where the thermal gradient was modest.

In several particles, SiC coatings had been damaged during fabrication and contributed an additional 6% failure of the SiC coatings in specimen 1D-1 and 9% in specimen 3A-1. Only one failed LTI outer coating was observed out of the 68 coated SAR particles examined, and it occurred on a particle that contained a defective SiC coating. Typical examples of particles that contained defective SiC coatings are shown in Fig. 41. Examination of the Biso-coated ThO_2 particles revealed no evidence of amoeba or indications of potential failure. A typical fertile coated particle is shown in Fig. 42.

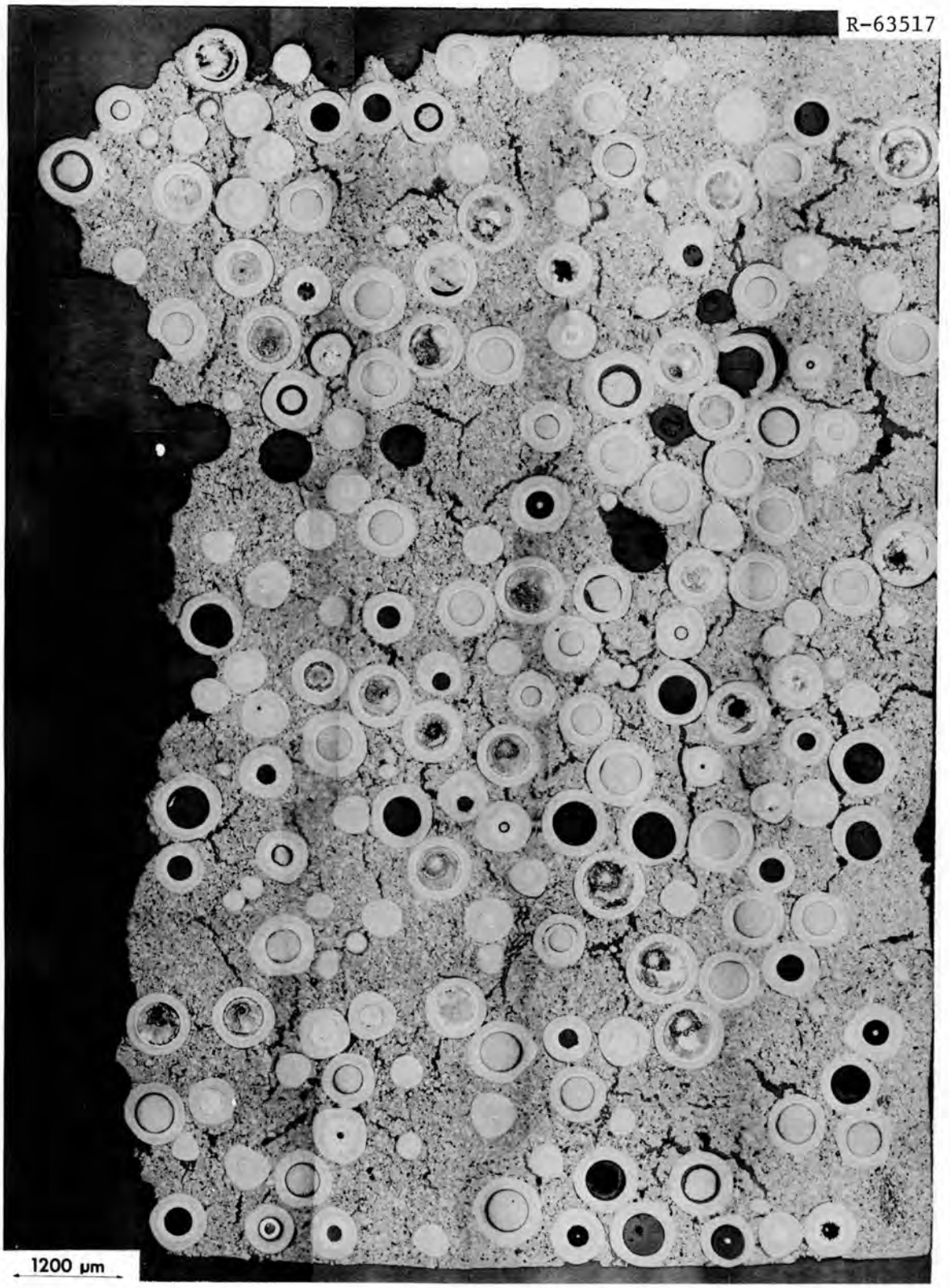

Fig. 38. Longitudinal Section Through P13N Specimen 1D-1.

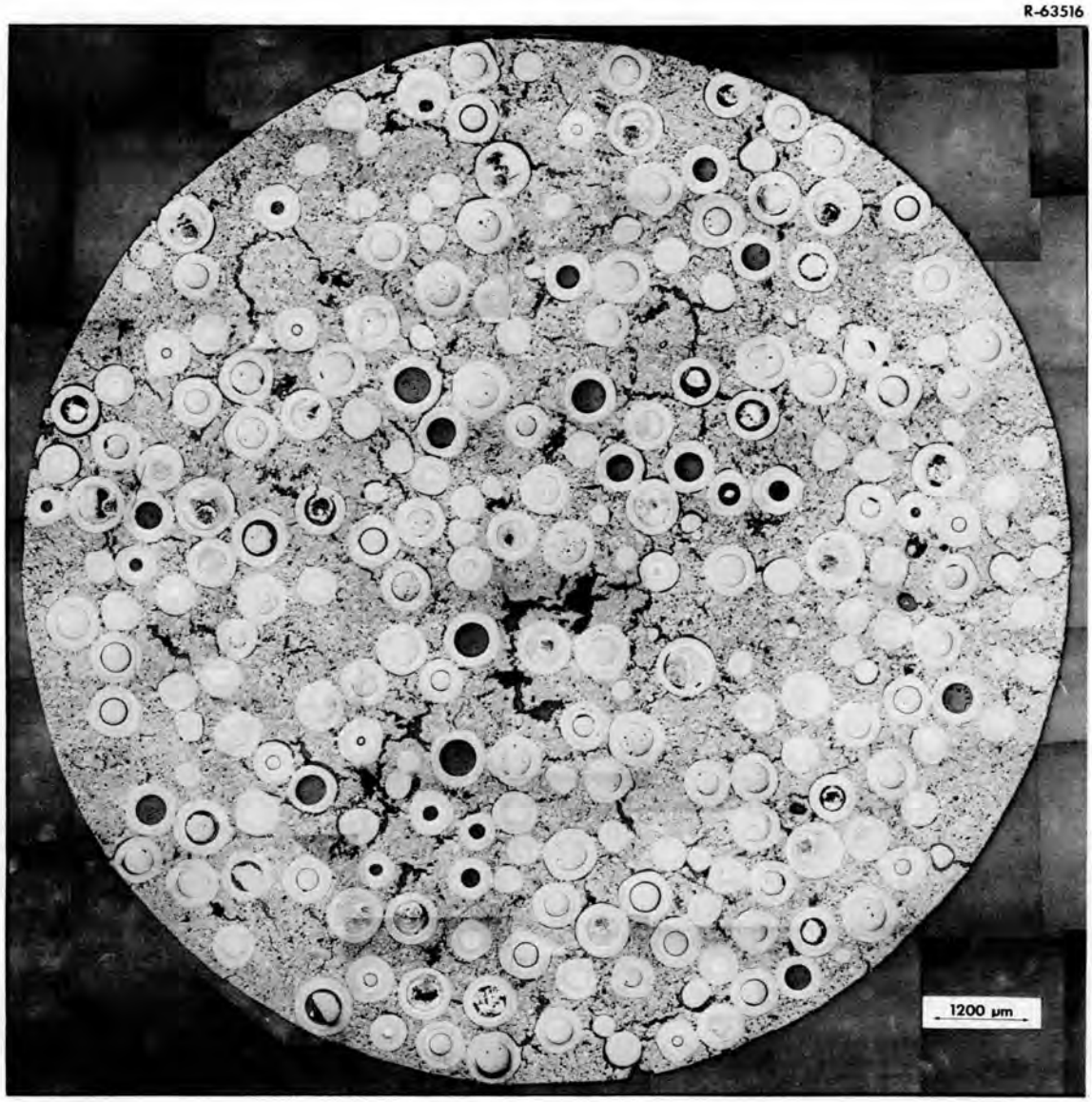

Fig. 39. Transverse Section through P13N Specimen

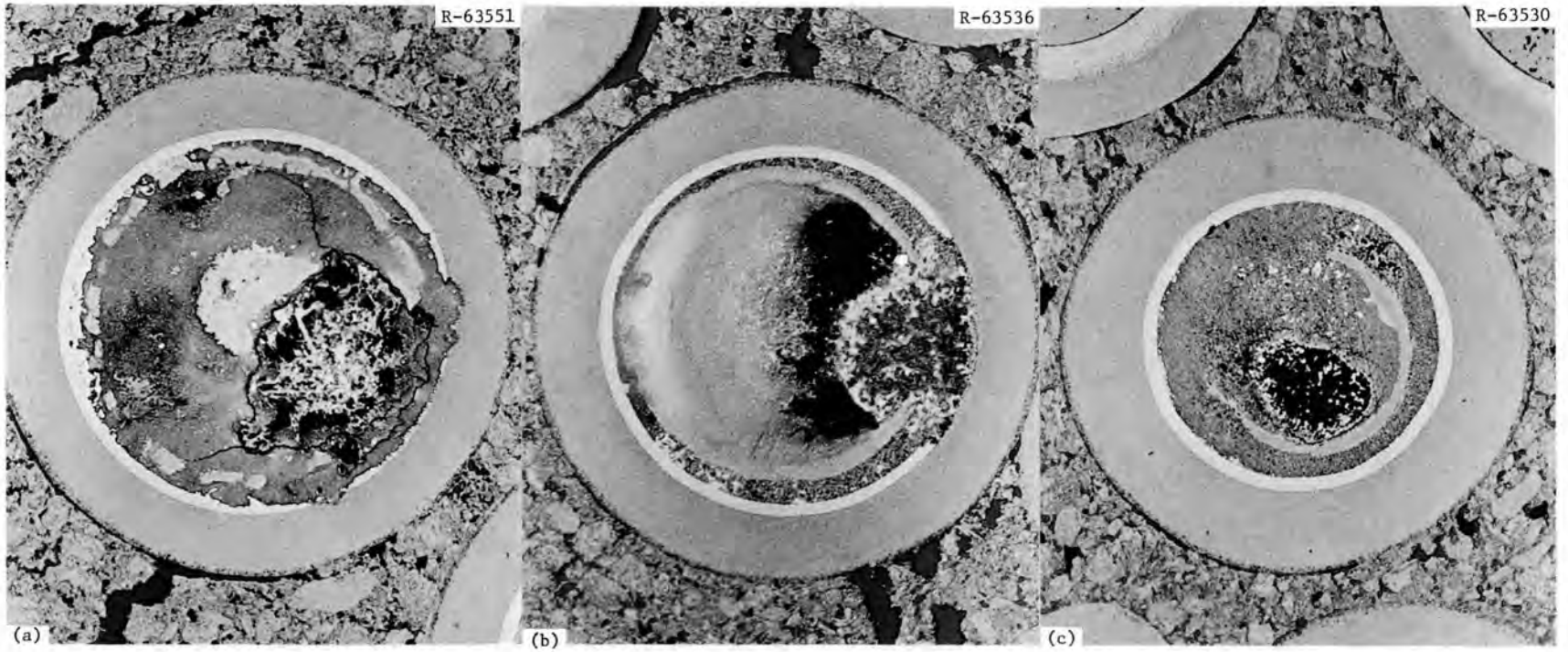

Fig. 40. Typical Microstructural Appearances of the Triso-Coated Strong Acid Resin Kernels after Irradiation. 150×, reduced 27%. (a) From near periphery of fuel rod 1D-1; (b) from near periphery of fuel rod 3A-1; and (c) from center of fuel rod 3A-1.

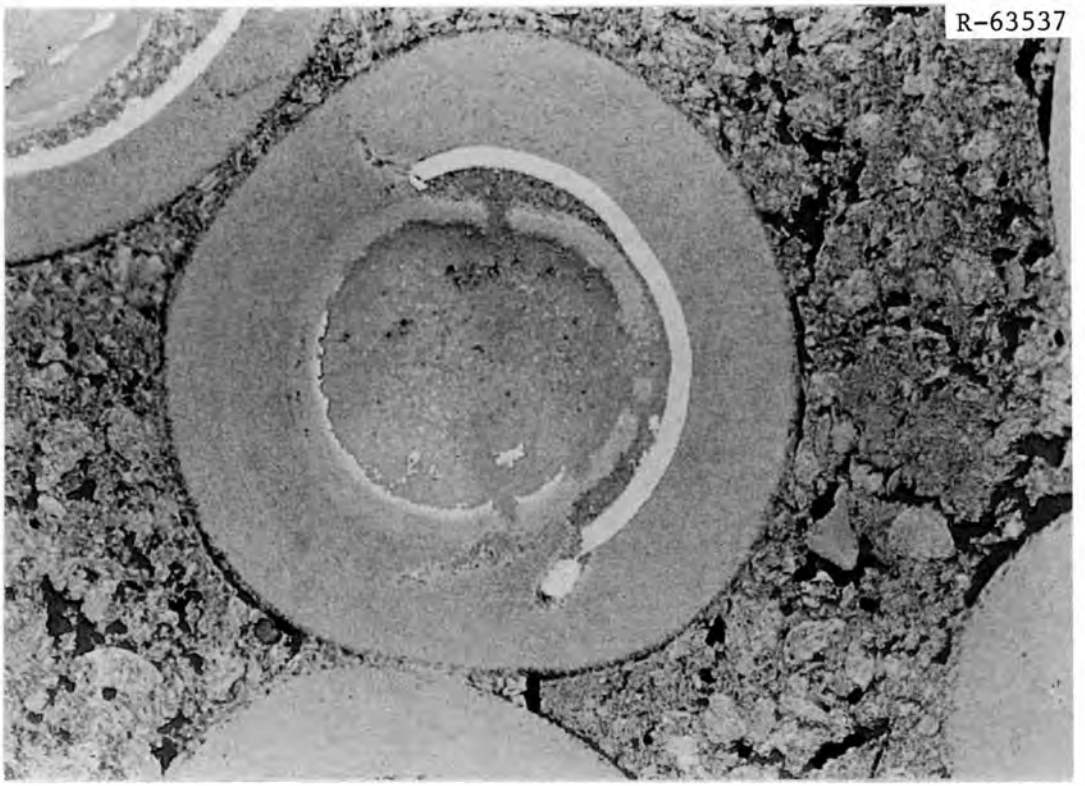

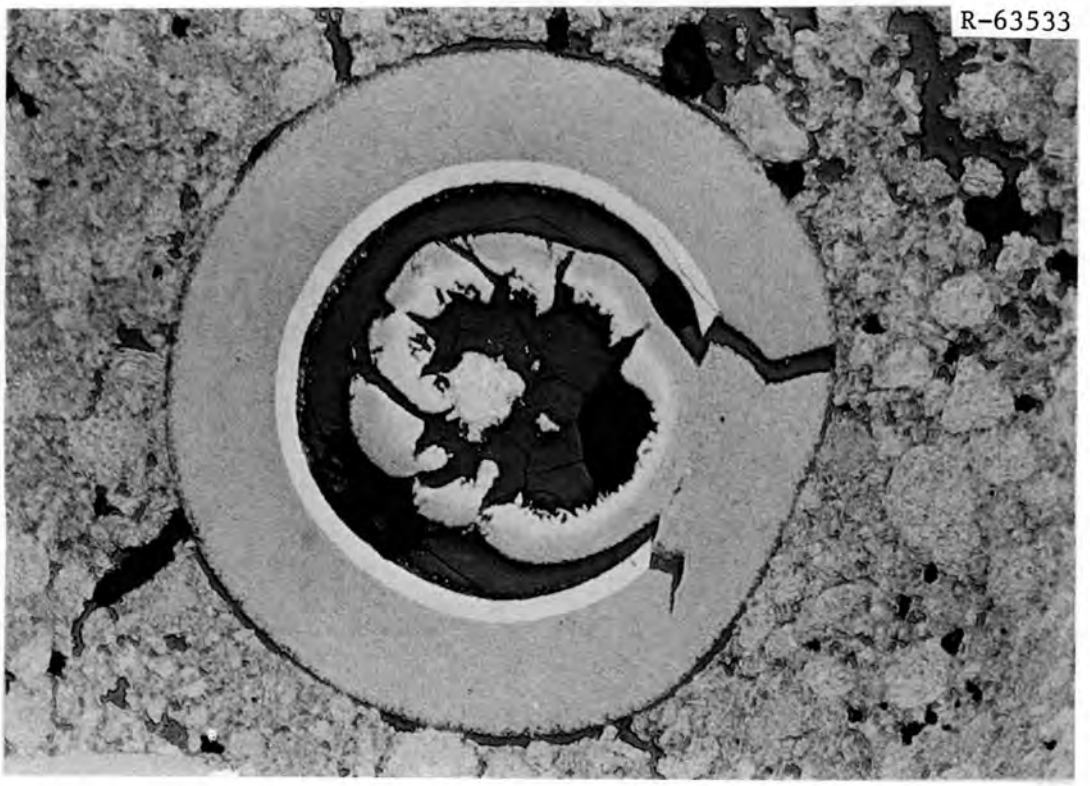

Fig. 41. Examples of Fabrication Defects found in Triso-Coated Strong-Acid-Resin Kernels in Fuel Rods 1D-1 and 3A-1. 150×.

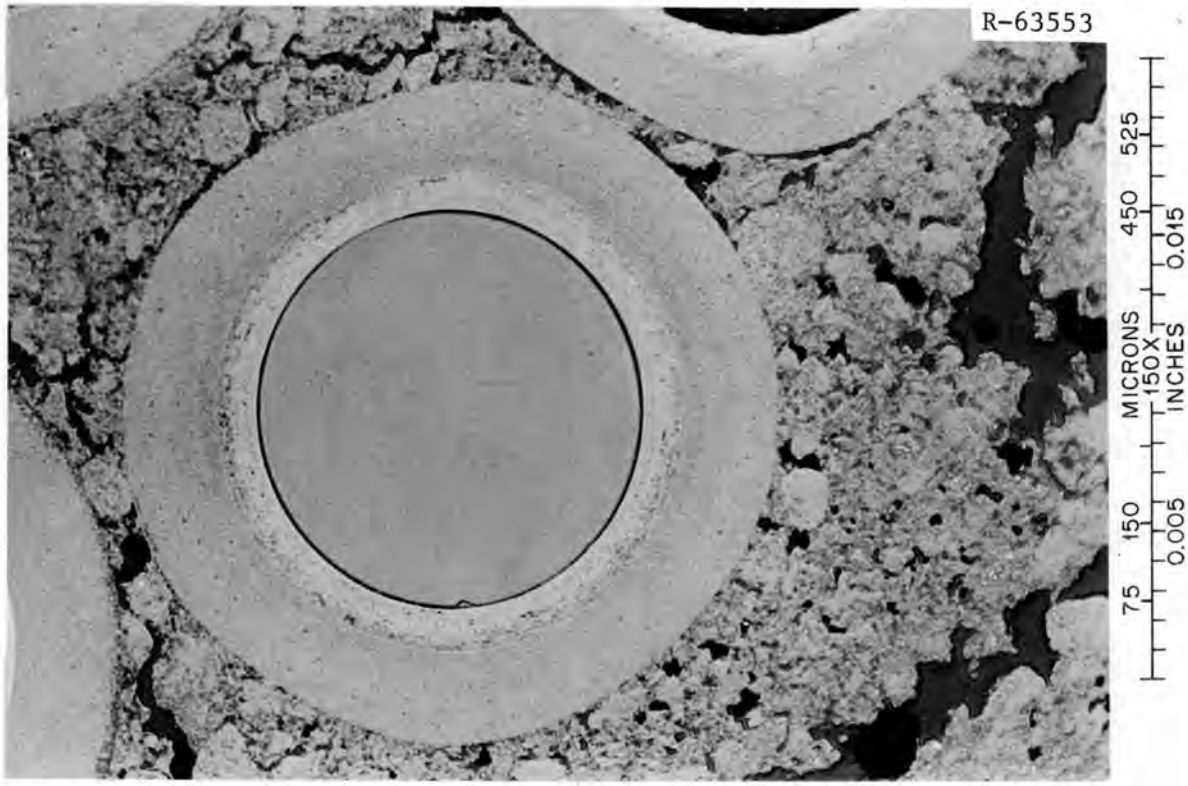

Fig. 42. Microstructures Typical of the Biso-Coated ThO_2 Kernels in Warm-Molded Fuel Rods after Irradiation in Capsule P13N.

Electron-Microprobe Analysis

The specimen that operated at the higher integrated temperature and fluence, 3A-1, was submitted for electron microprobe analysis. Coated fissile particles with both intact and failed SiC coatings were analyzed. The resulting characteristic x-ray images from uranium, sulfur, and silicon contained in intact and failed SiC coatings are shown in Figs. 43 and 44, respectively. The microprobe results confirmed that the silicon was dissolved from the hot side and rejected on the inner surface of the cold side of the SiC coating. Examination of the kernel disclosed that the uranium and sulfur did not segregate during migration up the thermal gradient. The x-ray images formed from the major metallic fission products, Fig. 45, did not show a concentration of the rare-earth fission products on the cooler side of the SiC coating, as has been reported in other coated-particle systems that have been exposed to a thermal gradient.[18] An obvious difference in the particles with failed SiC coatings was the absence of cesium and barium in the x-ray displays.

---

[18]Gulf General Atomic, *HTGR Base Program Quart. Progr. Rep. May 31, 1973*, Gulf-GA-A-12599, pp. 87–93.

Y-120898

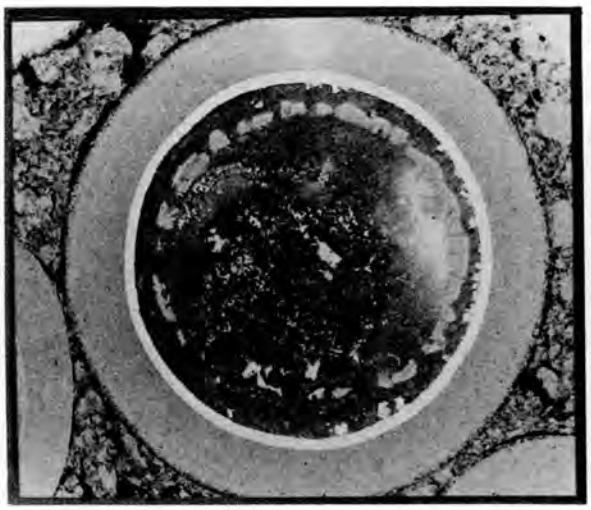

Optical

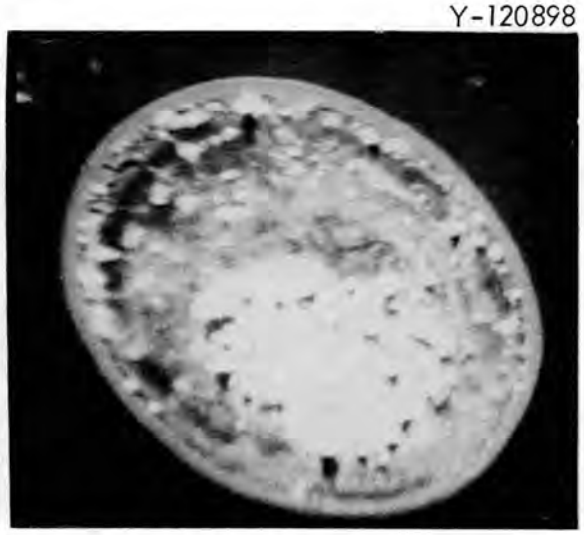

Backscattered Electrons

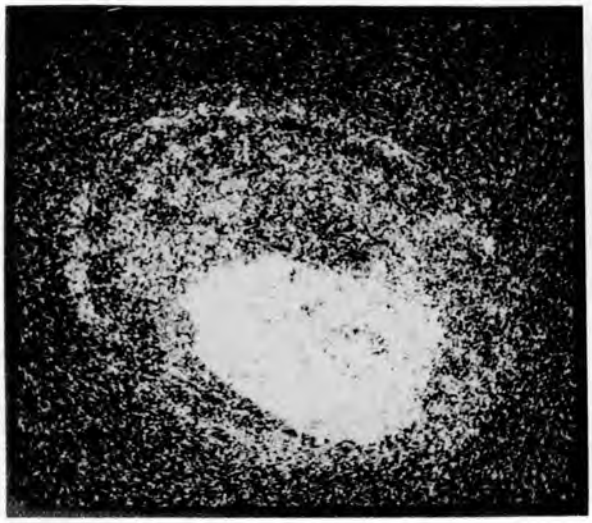

U Mβ

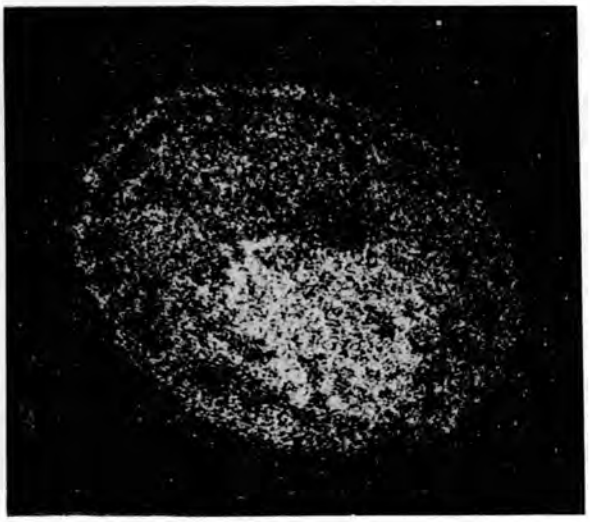

S Kα

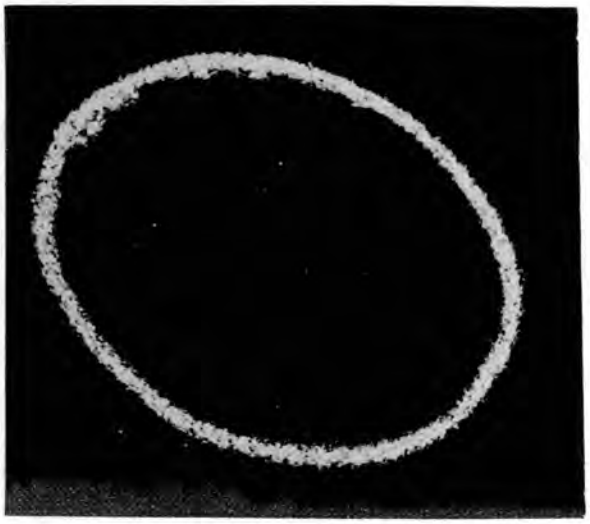

Si Kα

Fig. 43. Electron-Microprobe Analysis of an Intact Coated Strong-Acid-Resin Particle from Capsule P13N.

Y-120899

Optical

Backscattered Electrons

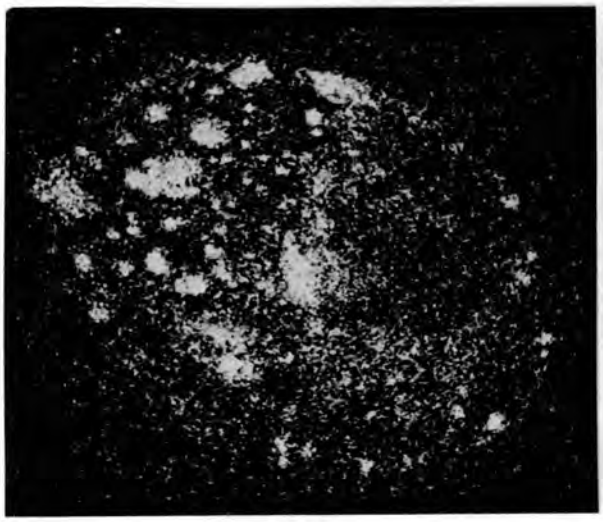

UMβ

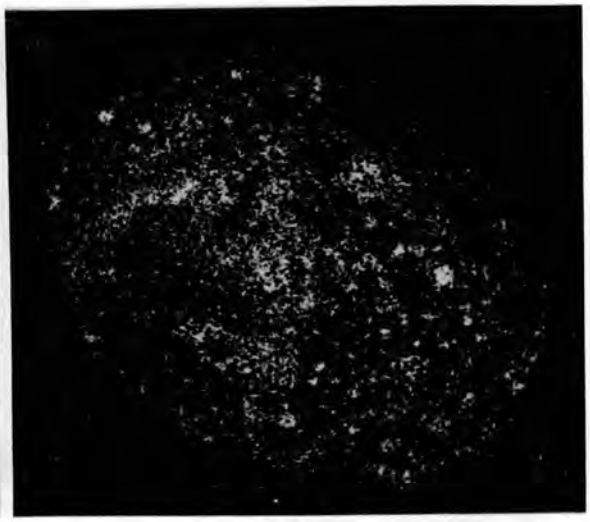

S Kα

Si Kα

Fig. 44. Electron-Microprobe Analysis of a Failed Coated Strong-Acid-Resin Particle from Capsule P13N.

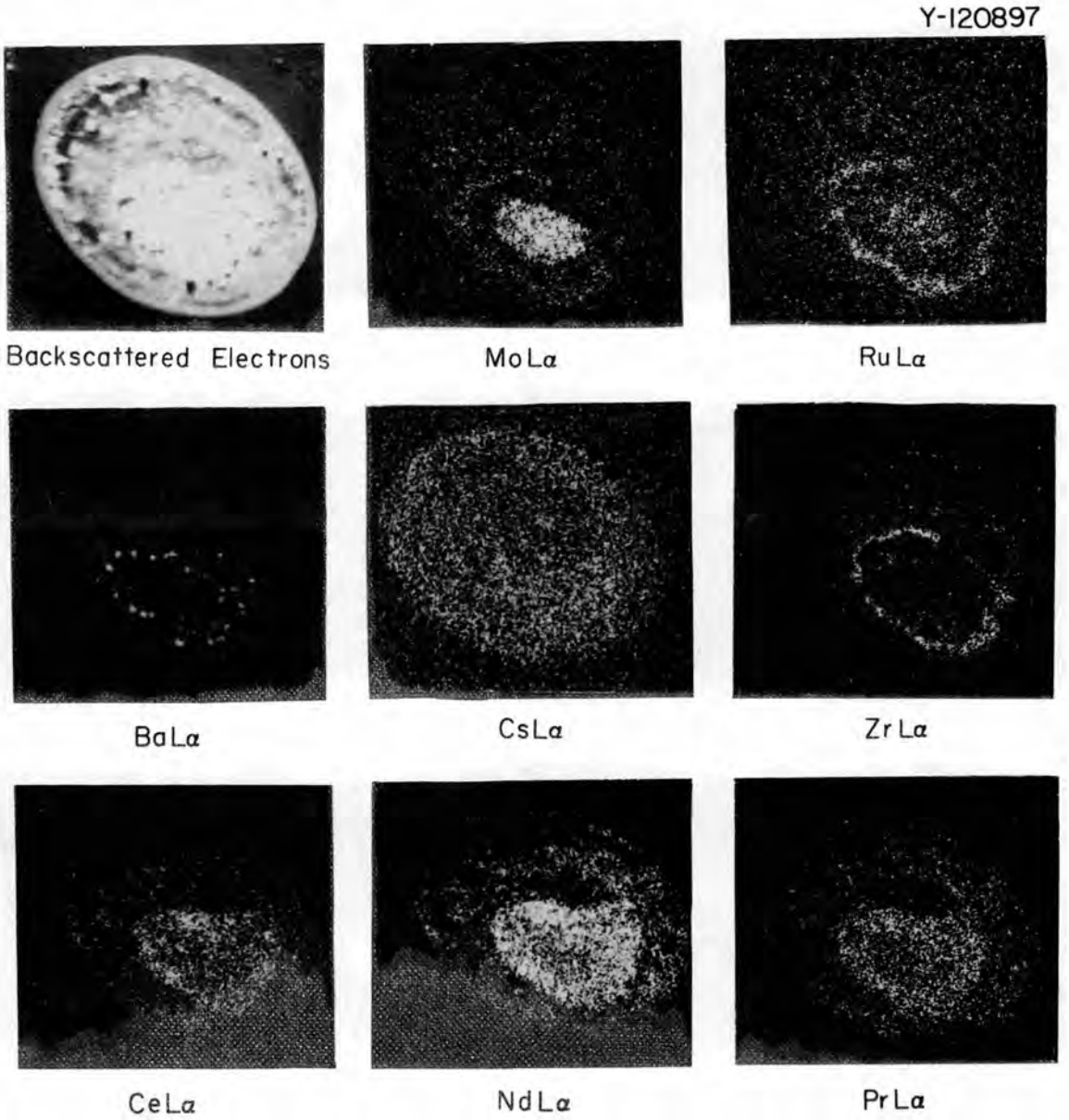

Fig. 45. Distribution of Fission Products in a Strong-Acid-Resin Kernel from Capsule P13N.

COMPARISON OF RESULTS IN HRB-3 AND P13N

It is instructive to compare the fissile and fertile particle performance in HRB-3 with that in P13N. Making the comparison, one must recognize that a considerable uncertainty exists in operating temperatures of samples in the two capsules. Consider the results shown in Table 14. The burnup of the fissile particles in HRB-3 was about 40% of that in P13N because of differences in enrichment of the uranium (7.35% ^{235}U in HRB-3, 90.8% ^{235}U in P13N). In both capsules the inner LTI coating failed in some particles and attack of the SiC coating was observed. In addition, distinct amoeba migration was observed in P13N due either to the high burnup or perhaps a higher operating temperature. In spite of the failure of the inner LTI coatings and attack of the SiC, very few outer coating failures were observed and fission-gas release was low throughout for P13N.

In direct contrast to the fissile particles, the fertile particles showed amoeba migration in HRB-3 and no migration in P13N. This difference is probably due to the much higher burnup in HRB-3 and suggests that a threshold burnup is required before amoeba migration begins. The influence of irradiation time on kernel migration is also a possible contributing factor to the differences observed between HRB-3 and P13N. The P13N experiment was irradiated for significantly less time than HRB-3. Possibly the ThO_2 in the P13N specimens would have migrated had the experiment been in-reactor longer. The complex relationship between temperature, temperature gradient, burnup, and time is now under careful study. Quantification of the relationship will require well-characterized irradiation data on real-time tests as well as accelerated tests such as HRB-3 and P13N.

DISCUSSION

The HRB-3 experiment marked several "firsts" for the ORNL HTGR fuels irradiation program. It was the first time HTGR fuel was irradiated in the HFIR with a center-line thermocouple. It was the first test of full-length fuel rods fabricated by the slug-injection method. Also, it was the first time "amoeba" was observed in reference fertile particles that operated at or near design conditions of temperature and heat rating.

In general, the ORNL fuel rod specimens irradiated in HRB-3 performed well. Stereo examination of the irradiated rods revealed a few broken particles. Metallographic examination revealed that the dense matrix of the warm-molded specimens was relatively unaffected by irradiation. The strong-acid-resin-derived fissile particles exhibited a variety of kernel structures after irradiation, and there was some attack of the inner isotropic coating and silicon carbide layers of the particles, but the attack did not lead to failures of the outer isotropic coating.

Perhaps the most significant observation made during metallographic examination of the HRB-3 specimens was the migration (amoeba) of the

Table 14. Comparative Results of Fuel Particles in HRB-3 and P13N

	Irradiation		Fissile Particles		Fertile Particles	
	Time-Averaged Fuel Center Temperature (°C)	Duration (Days)	Burnup (% FIMA)	Amoeba	Burnup (% FIMA)	Amoeba
HRB-3 Sample 3A	1450	253.8	26.5	No	15.0	Yes
P13N Sample 3A-1	1480	155.5	66.0	Yes	2.0	No

thoria kernels up the temperature gradient. This was the first time this behavior has been observed in ORNL irradiation experiments. Of the three specimens (1D, 1E, 3A) examined metallographically, amoeba of the fertile kernel was observed in two (1E and 3A). That this effect was not seen in specimen 1D, immediately adjacent to 1E is somewhat puzzling, although only one thoria particle was observed to have undergone amoeba in specimen 1E, and the amount of migration was too small to measure. Specimen 1E was somewhat closer to the reactor midplane, and therefore operated at higher heat rating and attained higher burnup. This behavior, coupled with the lack of thoria migration in previous HRB experiments of shorter duration, suggests a threshhold in both burnup and temperature for the onset of amoeba. Also it is suggested that once amoeba begins it proceeds rapidly, as significant migration was noted in specimen 3A.

The dimensional stability of the HRB-3 rods very closely approximates the behavior[19] of the Triso-Triso fuel irradiated in HRB-2. That the HRB-3 rods behaved like Triso-Triso fuel when the fertile particles were in fact Biso is probably due to the presence of Triso-coated inert particles. As indicated previously[19] Triso particles increase the dimensional stability of the rods because the silicon carbide layer provides an unyiel ing substrate, so only the change in thickness of the outer isotropic laye contributes to the dimensional changes observed in the fuel rods. Support for this conclusion is found in examining the dimensional change data of the rods irradiated in experiment P13N. These rods contained the same matrix material and same fissile and fertile particles as those irradiated in HRB-3, but did not contain the Triso inert particles. As shown in Fig. 24 (p. 29) the P13N rods shrank more than the HRB-3 fuel rods, but not as much as the Biso-Biso fuel irradiated[19] in HRB-2. The P13N rods operated hotter than rods in HRB-3.

CONCLUSIONS

The results of the HRB-3 and P13N experiments have shown that:

1. Warm-molded fuel rods containing 33 and 42 vol % particles performed well to full fast neutron exposure anticipated for commercial HTGRs. The dimensional stability of these rods was comparable to that of rods that contained only Triso-Triso particles. This comparison and the comparison of the P13N specimen dimensional changes with HRB-3 indicate that

---

[19] J. H. Coobs, J. L. Scott, B. H. Montgomery, J M Robbins, C. B. Pollock, and J. A. Conlin, *Irradiation Performance of HFIR Experiment HRB-2 of HTGR Fuel Sticks Bonded with Reference and Advanced Matrix Materials*, ORNL-TM-3988 (January 1973), p. 21.

the dimensional stability of a warm-molded fuel rod depends only weakly upon the volume fraction of particles.

2. Behavior of slug-injected fuel rods in HRB-2 and HRB-3 indicated that dimensional stability is strongly influenced by the particle system employed. Although there was little difference, if any, in the behavior of a Triso-Triso and a Triso-Biso system, there was a marked increase in shrinkage when a Biso-Biso system was used.

3. Slug-injected fuel rods also perform well to full fluence. The microstructure of these rods, which were carbonized in packed alumina, showed no signs of mechanical interaction between coated particle and matrix. But the matrix was very porous and discontinuous, so that it would contribute little to the conduction of heat away from the fuel particles.

4. Thoria fertile kernels migrate under certain conditions of time, temperature, temperature gradient, and burnup. The HRB-3 data, couples with data from other experiments, has suggested a threshhold for all four parameters. We are now attempting to define the threshhold values. Amoeba migration appears to occur rapidly after a threshhold has been passed.

5. Strong-acid-resin-derived fissile particles generally performed well under typical HTGR conditions, although chemical attack of the inner isotropic layer and silicon carbide layer by fuel compounds were pronounced in the P13N fuel rods. This attack was not correlated with temperature gradient in HRB-3 but was strongly correlated with temperature gradient in P13N. Further development of the strong-acid-resin system has been deemphasized until the reactions of sulfur-containing fuel are better understood.

ACKNOWLEDGMENTS

The authors wish to acknowledge the efforts of many people who made significant contributions to the planning, execution, and evaluation of these irradiation tests. We would like to acknowledge W. P. Eatherly for his help in planning these tests and in coordinating the fabrication of components in order to meet the irradiation schedules; R. A. Bradley and W. H. Miller, Jr., for fabricating and characterizing the slug-injected fuel rods; J M Robbins and D. E. Rosson for fabricating and characterizing the warm-molded fuel rods; all members of the Metals and Ceramics Division. The fissile and fertile particles were coated and characterized by C. B. Pollock, formerly with the Metals and Ceramics Division and now with the Materials Engineering Development Department, Y-12. The dosimetry and thermometry of the HRB-3 capsule were provided by H. T. Kerr of the Reactor Division and R. L. Shepard of the Instruments and Controls Division, respectively. The metallography of the unirradiated loose particles and fuel rods was performed by M. D. Allen of the General Metallography Group, and the remote metallography was performed by N. M. Atchley and L. G. Shrader of the Radiation and Electron Metallography Group of the Metals and Ceramics Division. The authors also acknowledge the assistance of those who helped with the preparation of this report, S. Peterson for technical editing and Regina Gossage for typing and makeup.

ORNL-TM-4526
(UC-77 Gas-Cooled
Reactor Technology)

INTERNAL DISTRIBUTION

(3) Central Research Library
ORNL — Y-12 Technical Library
Document Reference Section
(10) Laboratory Records Department
Laboratory Records, ORNL RC
ORNL Patent Office
R. G. Affel
S. E. Beall
R. L. Beatty
M. Bender
L. L. Bennett
E. S. Bettis
R. E. Blanco
A. L. Boch
E. S. Bomar
R. A. Bradley
R. E. Brooksbank
A. J. Caputo
J. M. Chandler
T. E. Cole
J. A. Conlin
(5) J. H. Coobs
W. H. Cook
D. Costanzo
W. B. Cottrell
J. A. Cox
F. L. Culler
J. E. Cunningham
F. C. Davis
H. J. de Nordwall
F. F. Dyer
W. P. Eatherly
R. B. Evans, III
J. I. Federer
G. G. Fee
D. E. Ferguson
R. B. Fitts
R. J. Gray
P. A. Haas
R. L. Hamner
J. W. Hill, Jr.
(3) M. R. Hill
(5) F. J. Homan
J. P. Jarvis
J. D. Jenkins
D. R. Johnson
M. J. Kania
(38) P. R. Kasten
H. T. Kerr
W. J. Lackey
K. H. Lin
T. B. Lindemer
E. L. Long, Jr.
A. L. Lotts
R. E. MacPherson
A. P. Malinauskas
H. C. McCurdy
W. T. McDuffee
B. H. Montgomery
M. T. Morgan
F. H. Neill
K. J. Notz
L. C. Oakes
P. Patriarca
R. L. Pearson
W. H. Pechin
C. B. Pollock (Y-12)
H. Postma
W. W. Proaps
J M Robbins
M. W. Rosenthal
P. Rubel
J. P. Sanders
C. D. Scott
J. L. Scott
J. D. Sease
J. H. Shaffer
R. L. Shephard
J. W. Snider
I. Spiewak
K. R. Thoms
M. Tobias
D. B. Trauger
V.C.A. Vaughen
K. H. Valentine
T. N. Washburn

J. R. Weir
J. C. White
R. G. Wymer
Walter Kohn (consultant)
W. C. Leslie (consultant)
John Moteff (consultant)
J. W. Prados (consultant)
G. V. Smith (consultant)

EXTERNAL DISTRIBUTION

USAEC DIVISION OF REACTOR RESEARCH AND DEVELOPMENT, Washington, DC 20545

(2) Director

USAEC OAK RIDGE OPERATIONS OFFICE, P.O. Box E, Oak Ridge, TN 37830

Director, Reactor Division
(2) Research and Technical Support Division

USAEC TECHNICAL INFORMATION CENTER, Office of Information Services, P.O. Box 62, Oak Ridge, TN 37830

(143) For distribution as shown in TID-4500 Distribution Category, UC-77, Gas-Cooled Reactor Technology

☆U. S. GOVERNMENT PRINTING OFFICE: 1974-748-189/66